

16 (Fig. 5). Since DNA double strand breaks (DSBs)-containing chromosome domains are mobile [39], the DNA fragment of chromosome 16 might migrate to the breakage site of chromosome 17 where the *red/gam* reporter genes are present. Although further investigations are required to reveal the precise mechanisms by which DNA rearrangements are induced by MMC, the results strongly suggest that GDL1 cells are useful to investigate the molecular mechanisms of translocations induced by chromosome instability.

An intriguing feature of GDL1 cells is the higher spontaneous frequencies in the  $\text{Spi}^-$  and *gpt* mutations compared to those of *gpt* delta mice (Tables 3 and 4). The spontaneous  $\text{Spi}^-$  MFs in *gpt* delta mice are  $1.1 \times 10^{-6}$  in epidermis [12],  $1.3 \times 10^{-6}$  to  $1.8 \times 10^{-6}$  in bone marrow [7,8],  $1.8 \times 10^{-6}$  in spleen,  $2.2 \times 10^{-6}$  in liver,  $2.4 \times 10^{-6}$  in testis, and  $2.6 \times 10^{-6}$  in kidney [9]. Since spontaneous MF of  $\text{Spi}^-$  selection in GDL1 cells was  $25.6 \times 10^{-6}$  (Table 3), it is 9.8–23-fold higher than the MFs in the organs of mice. Similarly, the spontaneous *gpt* MFs in *gpt* delta mice are  $2.4 \times 10^{-6}$  to  $6.6 \times 10^{-6}$  in liver [9,40],  $6.0 \times 10^{-6}$  in lung [41],  $6.2 \times 10^{-6}$  to  $9.0 \times 10^{-6}$  in colon [40,42],  $8.2 \times 10^{-6}$  in bone marrow [8],  $12.1 \times 10^{-6}$  in dermis, and  $13.4 \times 10^{-6}$  in epidermis [11]. The spontaneous MF of 6-TG selection in GDL1 cells was  $22.7 \times 10^{-6}$  (Table 4). The value is 1.7–9.5-fold higher than the MFs in various organs of *gpt* delta mice. In particular, the specific MF of class I mutations of  $\text{Spi}^-$  (large deletions of a size more than 1 kbp) was more than 40 times higher in vitro ( $4.2 \times 10^{-6}$ ) than in vivo ( $0.1 \times 10^{-6}$ ) (Table 3). Even when we eliminated all possible clonally expanded class I mutants (Fig. 4), the specific MF was still about 20 times higher in GDL1 cells than in *gpt* delta mice. Single base deletions, i.e., class III mutants, also are more than 10 times higher in vitro ( $18.5 \times 10^{-6}$ ) than in vivo ( $1.5 \times 10^{-6}$ ). Most large deletions and single base deletions are probably due to the nonhomologous end-joining of DSBs in DNA and slippage errors during DNA replication, respectively. Thus, we suggest that spontaneous DNA strand breaks and slippage errors are more frequently induced in vitro than in vivo. Higher rates of cell proliferation in vitro compared with in vivo may be one reason for the higher incidence of DSBs and slippage errors in GDL1 cells.

Likewise, differences between in vitro and in vivo were seen in single base insertions and single base deletions in the spontaneous *gpt* mutations (Table 4). Eleven of forty-six (24%) mutations were single base insertions or small deletions in spontaneous *gpt* mutants in GDL1 cells (Table 2), and seven of them (7/11 = 64%) occurred in the DNA sequence in the run of the identical nucleotide (Fig. 6). On the contrary, in the *gpt* delta

mice, 4 of 29 mutations (14%) were single base deletions, and the mutations were not observed in the run of the identical nucleotide [8]. Not only in our cell lines but also in other cell lines having different lambda shuttle vectors for detection of mutations, insertions/deletions tend to be higher than those observed in the transgenic animals from which the cells originated [43–45]. Therefore, higher induction of deletion/insertion mutations is generally observed in cell lines carrying lambda shuttle vectors compared with in vivo. This tendency is expected to affect the increase in spontaneous MF more severely in  $\text{Spi}^-$  selection than in 6-TG selection because  $\text{Spi}^-$  selection is more sensitive to deletion/insertion mutations than 6-TG selection. In fact, the increase in spontaneous MFs was higher in  $\text{Spi}^-$  selection (9.8–23-fold) than in 6-TG selection (1.7–9.5-fold) when compared between in vitro and in vivo as described above.

The combination of a lambda shuttle vector and a reporter gene is one of the most effective tools presently applicable for mutation analysis. Several cell lines have been established from TG mouse strains harboring the lambda vector system. Big Blue Rat2 [46], Big Blue mouse embryonic fibroblast cell lines [47], BBR/ME, BBR/OE, and BBR/MFib [48] are immortalized cell lines carrying *lacI* shuttle vectors. BBR1 and BBM1 are primary cultured cell lines from *lacI* transgenic mice [49]. EF1 is a cell line derived from *lacZ* transgenic mice [50]. However, the parent animals were insensitive to the MMC treatment or X-ray irradiation that effectively induces deletions [51,52]. Induction of large deletion mutations in these cells has not been reported. The sizes of the reporter genes are approximately 1 kbp in *lacI*, 3 kbp in *lacZ*, and 0.3 kbp in *cII* [2]. It may be difficult to detect large deletion mutations larger than the reporter genes. Additionally, highly predominant induction of base substitution mutations may hide an increase in deletion mutations because both the *lacI* and *lacZ* systems detect both point mutations and deletion mutations in a single selection system. Therefore, the result in the present study that GDL1 cells detected large deletion mutations suggests a distinct advantage.

It is common to use some agents that accelerate and/or accumulate mutations to establish a cell line from an animal tissue. A majority of the cell lines from the lambda vector TG rodent strains were established after treatment with strong mutagens for the purpose of immortalizing the cells. X-ray and benzo[*a*]pyrene were used for the Big Blue mouse embryonic fibroblast cell line [47]. *N*-Ethyl-*N*-nitrosourea was used for BBR/ME, BBR/OE, and BBR/MFib [48]. However, the SV40 T antigen gene was used to establish the GDL1 cells. This is the first attempt to apply the SV40 T antigen to the cell lines

for genotoxicity assays. Information on the biological functions of the SV40 T antigen may support better understanding of the responses of GDL1 cells to mutagens. The normal functions of p53 were lost in the CHL, CHO, and L5178Y tk<sup>+/−</sup> cells, which are commonly used in genotoxicity tests [53,54]. The dysfunction of p53 prevents the cells from apoptosis when the cells are damaged by mutagens. Since p53 plays an important role in DNA repair and genome stability, the dysfunction of the protein may increase the genetic damage by mutagens.

The present study demonstrates that the established GDL1 cell line detected large deletion mutations induced by MMC. The GDL1 cell is a useful tool for detecting various mutations including large deletion mutations, which covers all types of mutations induced in *gpt* delta mice. Although there are two differences in mutation spectra, i.e., single base substitution and complex rearrangement, between GDL1 cells and *gpt* delta mice after MMC treatment, the mutations detected in GDL1 cells are generally consistent with observations in *gpt* delta mice. A combination of GDL1 cell and gene targeting techniques, such as siRNA, knockout, or overexpression of target genes, may be an informative approach to understanding intracellular procedures involved in mutation and DNA repair.

### Acknowledgement

This work was supported by a grant-in-aid from the Japan Health Science Foundation (MI and TN).

### References

- [1] C.J. Shaw, J.R. Lupski, Implications of human genome architecture for rearrangement-based disorders: the genomic basis of disease, *Hum. Mol. Genet.* 13 (2004) 57–64.
- [2] T. Nohmi, T. Suzuki, K. Masumura, Recent advances in the protocols of transgenic mouse mutation assays, *Mutat. Res.* 455 (2000) 191–215.
- [3] J.A. Heddle, S. Dean, T. Nohmi, M. Boerrigter, D. Casciano, G.R. Douglas, B.W. Glickman, N.J. Gorelick, J.C. Mirsalis, H.J. Martus, T.R. Skopek, V. Thybaud, K.R. Tindall, N. Yajima, *In vivo* transgenic mutation assays, *Environ. Mol. Mutagen.* 35 (2000) 253–259.
- [4] T. Nohmi, M. Katoh, H. Suzuki, M. Matsui, M. Yamada, M. Watanabe, M. Suzuki, N. Horiya, O. Ueda, T. Shibuya, H. Ikeda, T. Sofuni, A new transgenic mouse mutagenesis test system using Spi<sup>−</sup> and 6-thioguanine selections, *Environ. Mol. Mutagen.* 28 (1996) 465–470.
- [5] J.A. Gossen, H.J. Martus, J.Y. Wei, J. Vijg, Spontaneous and X-ray-induced deletion mutations in a *LacZ* plasmid-based transgenic mouse model, *Mutat. Res.* 331 (1995) 89–97.
- [6] H. Louro, M.J. Silva, M.G. Boavida, Mutagenic activity of cisplatin in the *lacZ* plasmid-based transgenic mouse model, *Environ. Mol. Mutagen.* 40 (2002) 283–291.
- [7] N. Okada, K. Masumura, T. Nohmi, N. Yajima, Efficient detection of deletions induced by a single treatment of mitomycin C in transgenic mouse *gpt* delta using the Spi<sup>−</sup> selection, *Environ. Mol. Mutagen.* 34 (1999) 106–111.
- [8] A. Takeiri, M. Mishima, K. Tanaka, A. Shioda, O. Ueda, H. Suzuki, M. Inoue, K. Masumura, T. Nohmi, Molecular characterization of mitomycin C-induced large deletions and tandem-base substitutions in the bone marrow of *gpt* delta transgenic mice, *Chem. Res. Toxicol.* 16 (2003) 171–179.
- [9] K. Masumura, K. Kuniya, T. Kurobe, M. Fukuoka, F. Yatagai, T. Nohmi, Heavy-ion-induced mutations in the *gpt* delta transgenic mouse: comparison of mutation spectra induced by heavy-ion, X-ray, and gamma-ray radiation, *Environ. Mol. Mutagen.* 40 (2002) 207–215.
- [10] T. Nohmi, M. Suzuki, K. Masumura, M. Yamada, K. Matsui, O. Ueda, H. Suzuki, M. Katoh, H. Ikeda, T. Sofuni, Spi<sup>−</sup> selection: an efficient method to detect gamma-ray-induced deletions in transgenic mice, *Environ. Mol. Mutagen.* 34 (1999) 9–15.
- [11] M. Horiguchi, K. Masumura, H. Ikehata, T. Ono, Y. Kanke, T. Sofuni, T. Nohmi, UVB-induced *gpt* mutations in the skin of *gpt* delta transgenic mice, *Environ. Mol. Mutagen.* 34 (1999) 72–79.
- [12] M. Horiguchi, K.I. Masumura, H. Ikehata, T. Ono, Y. Kanke, T. Nohmi, Molecular nature of ultraviolet B light-induced deletions in the murine epidermis, *Cancer Res.* 61 (2001) 3913–3918.
- [13] D.C. Doll, R.B. Weiss, B.F. Issell, Mitomycin: ten years after approval for marketing, *J. Clin. Oncol.* 3 (1985) 276–286.
- [14] M. Tomasz, Y. Palom, The mitomycin bioreductive antitumor agents: cross-linking and alkylation of DNA as the molecular basis of their activity, *Pharmacol. Ther.* 76 (1997) 73–87.
- [15] M. Tomasz, R. Lipman, D. Chowdary, J. Pawlak, G.L. Verdine, K. Nakanishi, Isolation and structure of a covalent cross-link adduct between mitomycin C and DNA, *Science* 235 (1987) 1204–1208.
- [16] M. Tomasz, A.K. Chawla, R. Lipman, Mechanism of mono-functional and bifunctional alkylation of DNA by mitomycin C, *Biochemistry* 27 (1988) 3182–3187.
- [17] K.G. Suresh, R. Lipman, J. Cummings, M. Tomasz, Mitomycin C-DNA adducts generated by DT-diaphorase. Revised mechanism of the enzymatic reductive activation of mitomycin C, *Biochemistry* 36 (1997) 14128–14136.
- [18] Y. Palom, R. Lipman, S.M. Musser, M. Tomasz, A mitomycin-N<sup>6</sup>-deoxyadenosine adduct isolated from DNA, *Chem. Res. Toxicol.* 11 (1998) 203–210.
- [19] Y. Palom, M.F. Belcourt, S.M. Musser, A.C. Sartorelli, S. Rockwell, M. Tomasz, Structure of adduct X, the last unknown of the six major DNA adducts of mitomycin C formed in EMT6 mouse mammary tumor cells, *Chem. Res. Toxicol.* 13 (2000) 479–488.
- [20] H. Ariga, S. Sugano, Initiation of simian virus 40 DNA replication in vitro, *J. Virol.* 48 (1983) 481–491.
- [21] J.H. Bielas, J.A. Heddle, Proliferation is necessary for both repair and mutation in transgenic mouse cells, *Proc. Natl. Acad. Sci. U.S.A.* 97 (2000) 11391–11396.
- [22] G.J. Carr, N.J. Gorelick, Mutational spectra in transgenic animal research: data analysis and study design based upon the mutant or mutation frequency, *Environ. Mol. Mutagen.* 28 (1996) 405–413.
- [23] A.K. Basu, C.J. Hanrahan, S.A. Malia, S. Kumar, R. Bizanek, M. Tomasz, Effect of site-specifically located mitomycin C-DNA monoadducts on in vitro DNA synthesis by DNA polymerases, *Biochemistry* 32 (1993) 4708–4718.
- [24] V.-S. Li, H. Kohn, Studies on the bonding specificity for mitomycin C-DNA monoalkylation processes, *J. Am. Chem. Soc.* 113 (1991) 275–283.

- [25] N.S. Srikanth, A. Mudipalli, A.E. Maccubbin, H.L. Gurtoo, Mutations in a shuttle vector exposed to activated mitomycin C, *Mol. Carcinog.* 10 (1994) 23–29.
- [26] A.E. Maccubbin, A. Mudipalli, S.S. Nadadur, N. Ersing, H.L. Gurtoo, Mutations induced in a shuttle vector plasmid exposed to monofunctionally activated mitomycin C, *Environ. Mol. Mutagen.* 29 (1997) 143–151.
- [27] P.S. Jat, P.A. Sharp, Cell lines established by a temperature-sensitive simian virus 40 large-T-antigen gene are growth restricted at the nonpermissive temperature, *Mol. Cell. Biol.* 9 (1989) 1672–1681.
- [28] J.M. Ruppert, B. Stillman, Analysis of a protein-binding domain of p53, *Mol. Cell. Biol.* 13 (1993) 3811–3820.
- [29] R.S. Quartin, C.N. Cole, J.M. Pipas, A.J. Levine, The amino-terminal functions of the simian virus 40 large T antigen are required to overcome wild-type p53-mediated growth arrest of cells, *J. Virol.* 68 (1994) 1334–1341.
- [30] S.M. Morris, A role for p53 in the frequency and mechanism of mutation, *Mutat. Res.* 511 (2002) 45–62.
- [31] P.C. Hanawalt, Controlling the efficiency of excision repair, *Mutat. Res.* 485 (2001) 3–13.
- [32] S. Adimoolam, J.M. Ford, p53 and regulation of DNA damage recognition during nucleotide excision repair, *DNA Repair* 2 (2003) 947–954.
- [33] P.C. Hanawalt, J.M. Ford, D.R. Lloyd, Functional characterization of global genomic DNA repair and its implications for cancer, *Mutat. Res.* 544 (2003) 107–114.
- [34] K.K. Bowman, D.M. Sicard, J.M. Ford, P.C. Hanawalt, Reduced global genomic repair of ultraviolet light-induced cyclobutane pyrimidine dimers in simian virus 40-transformed human cells, *Mol. Carcinog.* 29 (2000) 17–24.
- [35] J.M. Ford, E.L. Baron, P.C. Hanawalt, Human fibroblasts expressing the human papillomavirus E6 gene are deficient in global genomic nucleotide excision repair and sensitive to ultraviolet irradiation, *Cancer Res.* 58 (1998) 599–603.
- [36] F. Yatagai, T. Kurobe, T. Nohmi, K. Masumura, T. Tsukada, H. Yamaguchi, K. Kasai-Eguchi, N. Fukunishi, Heavy-ion-induced mutations in the *gpt* delta transgenic mouse: effect of p53 gene knockout, *Environ. Mol. Mutagen.* 40 (2002) 216–225.
- [37] C. Zhu, K.D. Mills, D.O. Ferguson, C. Lee, J. Manis, J. Fleming, Y. Gao, C.C. Morton, F.W. Alt, Unrepaired DNA breaks in p53-deficient cells lead to oncogenic gene amplification subsequent to translocations, *Cell* 109 (2002) 811–821.
- [38] M. Honma, M. Izumi, M. Sakuraba, S. Tadokoro, H. Sakamoto, W. Wang, F. Yatagai, M. Hayashi, Deletion, rearrangement, and gene conversion; genetic consequences of chromosomal double-strand breaks in human cells, *Environ. Mol. Mutagen.* 42 (2003) 288–298.
- [39] J.A. Aten, J. Stap, P.M. Krawczyk, C.H. van Oven, R.A. Hoebe, J. Essers, R. Kanaar, Dynamics of DNA double-strand breaks revealed by clustering of damaged chromosome domains, *Science* 303 (2004) 92–95.
- [40] K. Masumura, Y. Totsuka, K. Wakabayashi, T. Nohmi, Potent genotoxicity of aminophenylnorharman, formed from non-mutagenic norharman and aniline, in the liver of *gpt* delta transgenic mouse, *Carcinogenesis* 24 (2003) 1985–1993.
- [41] A.H. Hashimoto, K. Amanuma, K. Hiyoshi, H. Takano, K. Masumura, T. Nohmi, Y. Aoki, In vivo mutagenesis induced by benzo[a]pyrene instilled into the lung of *gpt* delta transgenic mice, *Environ. Mol. Mutagen.* 45 (2005) 365–373.
- [42] K. Masumura, M. Horiguchi, A. Nishikawa, T. Umemura, K. Kanki, Y. Kanke, T. Nohmi, Low dose genotoxicity of 2-amino-3,8-dimethylimidazo[4,5-f]quinoxaline (MeIQx) in *gpt* delta transgenic mice, *Mutat. Res.* 541 (2003) 91–102.
- [43] C.N. Sprung, Y.P. Wang, D.L. Miller, D.D. Giannini, N. Dhananjaya, W.J. Bodell, Induction of *lacI* mutations in Big Blue Rat-2 cells treated with 1-(2-hydroxyethyl)-1-nitrosourea: a model system for the analysis of mutagenic potential of the hydroxyethyl adducts produced by 1,3-bis(2-chloroethyl)-1-nitrosourea, *Mutat. Res.* 484 (2001) 77–86.
- [44] D.M. Zimmer, X.B. Zhang, P.R. Harbach, J.K. Mayo, C.S. Aaron, Spontaneous and ethylnitrosourea-induced mutation fixation and molecular spectra at the *lacI* transgene in the Big Blue rat-2 embryo cell line, *Environ. Mol. Mutagen.* 28 (1996) 325–333.
- [45] J.C. Ryu, Y.J. Kim, Y.G. Chai, Mutation spectrum of 1,2-dibromo-3-chloropropane, an endocrine disruptor, in the *lacI* transgenic Big Blue Rat2 fibroblast cell line, *Mutagenesis* 17 (2002) 301–307.
- [46] D.L. Wyborski, S. Malkhosyan, J. Moores, M. Perucho, J.M. Short, Development of a rat cell line containing stably integrated copies of a lambda/*lacI* shuttle vector, *Mutat. Res.* 334 (1995) 161–165.
- [47] G.L. Erexson, M.L. Cunningham, K.R. Tindall, Cytogenetic characterization of the transgenic Big Blue Rat2 and Big Blue mouse embryonic fibroblast cell lines, *Mutagenesis* 13 (1998) 649–653.
- [48] H.M. McDiarmid, G.R. Douglas, B.L. Coomber, P.D. Josephy, Epithelial and fibroblast cell lines cultured from the transgenic BigBlue rat: an in vitro mutagenesis assay, *Mutat. Res.* 497 (2001) 39–47.
- [49] G.L. Erexson, D.E. Watson, K.R. Tindall, Characterization of new transgenic Big Blue<sup>®</sup> mouse and rat primary fibroblast cell strains for use in molecular toxicology studies, *Environ. Mol. Mutagen.* 34 (1999) 90–96.
- [50] P.A. White, G.R. Douglas, J. Gingerich, C. Parfett, P. Shwed, V. Seligy, L. Soper, L. Berndt, J. Bayley, S. Wagner, K. Pound, D. Blakey, Development and characterization of a stable epithelial cell line from Muta Mouse lung, *Environ. Mol. Mutagen.* 42 (2003) 166–184.
- [51] T. Suzuki, M. Hayashi, T. Sofuni, B.C. Myhr, The concomitant detection of gene mutation and micronucleus induction by mitomycin C in vivo using *lacZ* transgenic mice, *Mutat. Res.* 285 (1993) 219–224.
- [52] K.S. Tao, C. Urlando, J.A. Heddle, Comparison of somatic mutation in a transgenic versus host locus, *Proc. Natl. Acad. Sci. U.S.A.* 90 (1993) 10681–10685.
- [53] T. Hu, C.M. Miller, G.M. Ridder, M.J. Aardema, Characterization of p53 in Chinese hamster cell lines CHO-K1, CHO-WBL, and CHL: implications for genotoxicity testing, *Mutat. Res.* 426 (1999) 51–62.
- [54] R.D. Storer, A.R. Kraynak, T.W. McKelvey, M.C. Elia, T.L. Goodrow, J.G. DeLuca, The mouse lymphoma L5178Y Tk<sup>+/−</sup> cell line is heterozygous for a codon 170 mutation in the p53 tumor suppressor gene, *Mutat. Res.* 373 (1997) 157–165.

## In Vivo Mutagenesis in the Lungs of *gpt*-delta Transgenic Mice Treated Intratracheally With 1,6-Dinitropyrene

Akiko H. Hashimoto,<sup>1</sup> Kimiko Amanuma,<sup>1</sup> Kyoko Hiyoshi,<sup>1,2</sup>  
Hirohisa Takano,<sup>1</sup> Ken-ichi Masumura,<sup>3</sup> Takehiko Nohmi,<sup>3</sup> and Yasunobu Aoki<sup>1\*</sup>

<sup>1</sup>Research Center for Environmental Risk, National Institute for Environmental Studies, Ibaraki, Japan

<sup>2</sup>Graduate School of Comprehensive Human Sciences, University of Tsukuba, Ibaraki, Japan

<sup>3</sup>Division of Genetics and Mutagenesis, National Institute of Health Sciences, Tokyo, Japan

1,6-Dinitropyrene (1,6-DNP) is a ubiquitous airborne pollutant found in diesel exhaust. In this study, mutagenesis was examined in the lungs of *gpt*-delta transgenic mice after intratracheal instillation of 0–0.1 mg 1,6-DNP. In addition, the 1,6-DNP-induced *gpt* mutation spectrum was compared with that of control mice. A single intratracheal injection of 0–0.05 mg 1,6-DNP resulted in significant dose-dependent increases in mutant frequency; the induced mutant frequency declined at the 0.1 mg dose. The average lung mutant frequencies at doses of 0.025, 0.05, and 0.1 mg 1,6-DNP were 2.9-, 4.1-, and 1.9-times higher than for control mice ( $(0.50 \pm 0.16) \times 10^{-5}$ ). The

major mutations induced by 1,6-DNP included G:C→A:T transitions, G:C→T:A transversions, and 1-base deletions. Among the G:C→A:T transitions isolated from 1,6-DNP-treated mice, five (at nucleotide positions 64, 110, 115, 116, and 418) were observed in four or more animals. These positions therefore are potential hotspots for 1,6-DNP mutation. The predominant frameshift mutations following 1,6-DNP treatment included single base pair deletions at G:C (9/13 = 69%). The results of this study indicate that 1,6-DNP is mutagenic for the lungs of mice. *Environ. Mol. Mutagen.* 47:277–283, 2006. © 2006 Wiley-Liss, Inc.

**Key words:** 1,6-dinitropyrene; *gpt*-delta transgenic mouse; 6-thioguanine selection

### INTRODUCTION

Suspended particulate matter in diesel exhaust (DE) is a suspected cause of lung cancer and allergic respiratory disease, including bronchial asthma [Muranaka et al., 1986]. Various potent carcinogens and mutagens, such as polycyclic aromatic hydrocarbons (PAHs) and nitrated PAHs, have been identified in DE particles [Harris, 1983]. Some of the compounds in DE, for instance, benzo[*a*]pyrene (B[*a*]P) and dinitropyrenes (DNPs), are pulmonary carcinogens in animals [Tokiwa et al., 1984; Brightwell et al., 1986; Jeffrey et al., 1990]. Among the DNPs, 1,6-DNP-induced lung tumors were detected in 50% of BALB/c mice after 112 days of s.c. inoculation [Tokiwa et al., 1984]. Following intratracheal instillation of 1,6-DNP, 90–100% of hamsters developed lung carcinomas along with myeloid leukemias [Takayama et al., 1985]. Iwagawa et al. [1989] showed that direct pulmonary instillation of 1,6-DNP led to lung tumors in Fischer 344 rats, and mutations in *K-ras* codon 12 were observed in the tumors induced in rat lungs using a similar dosing protocol [Smith et al., 1997]. Also, DNA adduct formation and gene mutation were analyzed in F344 rats in

which 1,6-DNP was directly administered to the lungs by implantation. A significant increase in *Hprt* gene mutations was detected in spleen T-lymphocytes [Smith et al., 1995].

Earlier in vitro assay results indicated that DNPs are potent mutagens. In the Salmonella mutation assay (Ames test), DNPs display strong mutagenicity without an exogenous metabolic activation system and predominantly induce frameshift-type mutations [Mermelstein et al., 1981; Sugimura and Takayama, 1983; Tokiwa et al.,

Grant sponsor: Japan Society for the Promotion of Sciences; Grant Number: 14207100.

\*Correspondence to: Yasunobu Aoki, National Institute for Environmental Studies, 16-2 Onogawa, Tsukuba, Ibaraki 305-8506, Japan. E-mail: ybaoki@nies.go.jp

Received 22 September 2005; provisionally accepted 7 October 2005; and in final form 6 January 2006

DOI 10.1002/em.20204

Published online 17 February 2006 in Wiley InterScience (www.interscience.wiley.com).

1984]. Salmeen et al. [1984] showed that mono- and dinitro-PAHs, which include 1,3-, 1,6-, and 1,8-DNP, 1-nitropyrene, and 3- and 8-nitrofluoranthene, account for 30–40% of the direct bacterial mutagenic activity of extracts from DE particulate. 1,6-DNP and 1,8-DNP are activated by nitroreduction and *O*-acetylation in bacteria to form DNA adducts [Rosenkranz and Mermelstein, 1983]. Following a single i.p. injection of 1,6-DNP into mice, this mutagen binds to lung DNA as 1-*N*-(deoxyguanosin-8-yl) amino-6-nitropyrene [Delclos et al., 1987]. The same guanine adduct also was formed in rat lungs instilled with 1,6-DNP [Smith et al., 1995]. The *in vivo* mutagenicity and mutation spectrum of 1,6-DNP in the lung, a target organ for air pollutants, should be useful for elucidating its carcinogenic mechanism of action. Oral administration of 1,3-, 1,6-, and 1,8-DNP mixtures leads to *in vivo* mutagenicity in MutaMouse<sup>®</sup> [Kohara et al., 2002]. However, the mutagenic effects of 1,6-DNP in the lung remain to be determined.

To estimate the *in vivo* mutagenicity of 1,6-DNP in the lung, we used the *gpt*-delta transgenic mouse [Nohmi et al., 1996; Thybaud et al., 2003]. These mice carry a  $\lambda$  phage EG10 transgene that includes the guanine phosphoribosyltransferase (*gpt*) gene. When the rescued phages are infected into *E. coli* expressing Cre recombinase, phage DNA is converted into plasmids harboring a gene for chloramphenicol (Cm) resistance (*cat*) and the *gpt* gene. The *gpt* mutants are detected as colonies arising on plates containing Cm and 6-thioguanine (6-TG). In this study, the mutant frequency and mutation spectrum obtained from the lungs of *gpt*-delta mice were examined after intratracheal instillation of 1,6-DNP. Mutant frequency in the lung increased in the presence of 0–0.05 mg 1,6-DNP. The predominant mutations induced by 1,6-DNP were G:C→A:T transitions, G:C→T:A transversions, and single-base deletions at C:G sites. Specifically, *gpt* nucleotides no. 64, 110, 115, 116, and 418 appeared to be mutation hotspots.

## MATERIALS AND METHODS

### Treatment of Mice

Twelve male *gpt*-delta mice were obtained from Japan SLC (Shizuoka, Japan). These mice carry about 80 copies of  $\lambda$  EG10 DNA on chromosome 17 in a C57BL/6J background [Nohmi et al., 1996]. Doses of 1,6-DNP (Sigma-Aldrich Japan, Tokyo, Japan) dissolved in tricapylin  $[(CH_3(CH_2)_6COOCH_2)_2CHOCO(CH_2)_6CH_3]$  (Sigma-Aldrich, St Louis, MO) were administered to each of three 9-week-old mice via a single intratracheal instillation. The animals were anesthetized with 4% halothane (Hoechst Japan, Tokyo, Japan) until the animal did not respond to a tactile stimulus. The animal was placed on a restraining board with linen threads to hold the mouth open. The 1,6-DNP solution was instilled into the trachea via a polyethylene tube [Takano et al., 2002; Hashimoto et al., 2005]. Two doses (0.025 and 0.05 mg) of 1,6-DNP were dissolved in 50  $\mu$ l tricapylin, while the 0.1 mg dose was dissolved in 100  $\mu$ l tricapylin. Three mice were treated with 50  $\mu$ l tricapylin alone as con-

trols. Mice were killed 14 days after 1,6-DNP treatment, which a previous study [Suzuki et al., 1999] indicated was sufficient for mutant manifestation in the lung. Their lungs were removed, frozen in liquid nitrogen, and stored at  $-80^\circ\text{C}$  until DNA isolation.

### *gpt* Mutation Assay

The *gpt* assay was performed as described previously [Nohmi et al., 2000]. High molecular weight genomic DNA was extracted from the pooled lung tissue from each animal, using the RecoverEase DNA isolation kit (Stratagene, La Jolla, CA).  $\lambda$  EG10 phages were rescued using Transpack packaging extract (Stratagene). To convert phage DNA into plasmids, *E. coli* YG6020 expressing Cre recombinase was infected with phage. Bacteria were spread onto M9 salt plates containing Cm and 6-TG [Nohmi et al., 2000], and incubated for 72 hr at  $37^\circ\text{C}$  for selection of colonies harboring a plasmid carrying the Cm acetyltransferase (*cat*) gene and a mutated *gpt* gene. The 6-TG-resistant colonies were streaked onto selection plates for confirmation of the resistant phenotype. Cells were cultured in LB broth containing 25  $\mu\text{g}/\text{ml}$  Cm at  $37^\circ\text{C}$  and collected by centrifugation. Bacterial pellets were stored at  $-80^\circ\text{C}$  until sequencing analysis.

### PCR and DNA Sequence Analysis of 6-TG-mutants

A 739-bp DNA fragment containing the *gpt* gene was amplified by PCR using primer-1 and primer-2, as described previously [Nohmi et al., 2000; Hashimoto et al., 2005]. The reaction mixture contained 5 pmol of each primer, and was 200 mM for each dNTP. PCR was performed using Ex *Taq* DNA polymerase (Takara Bio, Shiga, Japan) with a PTC-100 Thermal Cycler (MJ Research, Waltham, MA). The reaction mixture was incubated at  $94^\circ\text{C}$  for 4.5 min, followed by 30 cycles of 30 sec at  $94^\circ\text{C}$ , 30 sec at  $58^\circ\text{C}$ , and 1 min at  $72^\circ\text{C}$ . The last step was extended for 5 min at  $72^\circ\text{C}$ . After purification, amplified products were sequenced with a Big Dye Terminator v3.1 Cycle sequencing kit (Applied Biosystems, Foster City, CA) and an Applied Biosystems model 3730xl DNA analyzer. The sequencing oligonucleotides, primer-A and primer-C, are given in earlier reports [Nohmi et al., 2000; Hashimoto et al., 2005].

### Statistical Analysis

All data are expressed as mean  $\pm$  SD. The statistical significance of the mutant frequency data was analyzed using ANOVA and the Tukey post-hoc test. Data were considered statistically significant at  $P < 0.05$ . To evaluate the mutant frequency dose response, simple linear regression was performed. Mutational spectra were compared using the Adams-Skopek test [Adams and Skopek, 1987; Cariello et al., 1994].

## RESULTS

### 1,6-DNP-Induced *gpt* Mutations in the Lung

To examine the mutagenic effects of 1,6-DNP in the lung, *gpt*-delta transgenic mice were exposed to increasing doses of 1,6-DNP (0.025, 0.05, and 0.1 mg/mouse) by intratracheal instillation (Fig. 1). The mutant frequency in the lungs of control mice was  $(0.5 \pm 0.2) \times 10^{-5}$  (Table I). The mutant frequencies in control mice in this study were similar to those observed previously in several tissues of *gpt*-delta mice [Masumura et al., 1999, 2000, 2003; Hashimoto et al., 2005]. Single injections of 0.025, 0.05, and 0.1 mg 1,6-DNP resulted in 2.9-, 4.1-, and 1.9-

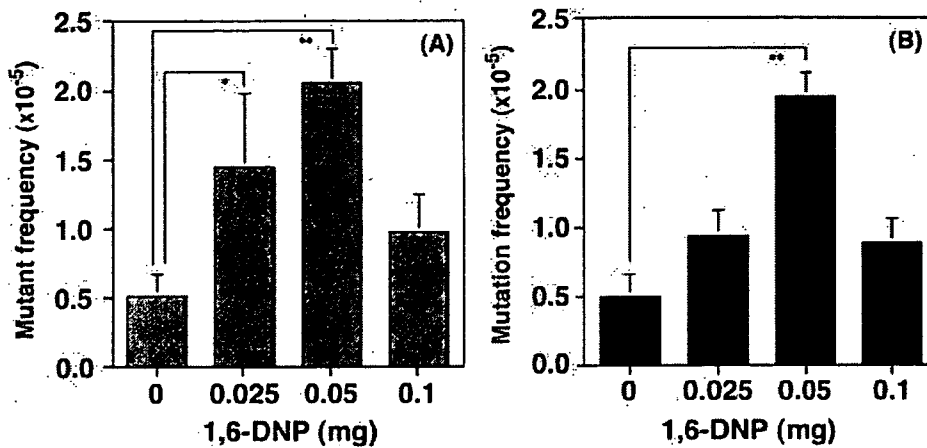


Fig. 1. 6-TG-resistant mutant frequency (A) and mutation frequency (B) in 1,6-DNP-treated *gpt*-delta mice. Data are presented as mean  $\pm$  SD. Statistical significance was determined using ANOVA and Tukey tests. Significant differences between control and 1,6-DNP-induced groups are indicated (\* $P < 0.05$ , \*\* $P < 0.01$ ).

TABLE I. Summary of Mutant and Mutation Frequencies in the Lungs of *gpt*-delta Mice After 1,6-DNP Treatment<sup>a</sup>

1,6-DNP amount (mg)	ID of animals	Number of colonies		Mutant frequency ( $10^{-5}$ )	Average mutant frequency $\pm$ SD ( $10^{-5}$ )	% independent mutations	Mutation frequency ( $10^{-5}$ )	Average mutation frequency $\pm$ SD ( $10^{-5}$ )
		Mutant	Total					
Control	1	3	441,600	0.68	$0.50 \pm 0.16$	100	0.68	$0.50 \pm 0.16$
	2	3	643,200	0.47		100	0.47	
	3	3	828,000	0.36		100	0.36	
	Total	9	1,912,800					
0.025	1	7	608,000	1.15	$1.45 \pm 0.53^b$	83	0.96	$0.94 \pm 0.18$
	2	9	800,000	1.13		67	0.75	
	3	13	630,400	2.06		54	1.11	
	Total	29	2,038,400					
0.05	1	15	652,800	2.30	$2.05 \pm 0.25^c$	91	2.10	$1.92 \pm 0.15^c$
	2	9	502,400	1.79		100	1.79	
	3	14	678,400	2.06		91	1.88	
	Total	38	1,833,600					
0.1	1	12	953,600	1.26	$0.96 \pm 0.28$	83	1.05	$0.89 \pm 0.18$
	2	7	1,000,000	0.70		100	0.70	
	3	5	536,000	0.93		100	0.93	
	Total	24	2,489,600					

<sup>a</sup>Statistical significance was determined using ANOVA test and Tukey test. Significant differences between the control and 1,6-DNP treated groups are indicated.

<sup>b</sup> $P < 0.05$ .

<sup>c</sup> $P < 0.01$ .

fold increases in mutant frequency ( $(1.5 \pm 0.5) \times 10^{-5}$ ,  $(2.1 \pm 0.3) \times 10^{-5}$ , and  $(1.0 \pm 0.3) \times 10^{-5}$ ) and 1.9-, 3.8-, and 1.8-fold increases in mutation frequency ( $(0.9 \pm 0.2) \times 10^{-5}$ ,  $(1.9 \pm 0.2) \times 10^{-5}$ , and  $(0.9 \pm 0.2) \times 10^{-5}$ ), compared with that in control mice, respectively. Mutant frequency was significantly increased at doses of 0.025 and 0.05 mg 1,6-DNP, but not at a dose of 0.1 mg 1,6-DNP. The mutation frequencies in these mice, calculated by correcting the mutant frequencies for the independence of the mutants determined by DNA sequencing (see below), are also shown in Table I and Figure 1.

#### Characteristics of the *gpt* Mutant Spectrum in 1,6-DNP-Treated Mice

To determine the mutation spectrum induced by 1,6-DNP in the lung, 99 *gpt* mutants from the lungs of treated and control mice were subjected to DNA sequencing analysis (Table II, Fig. 2). G:C→A:T transitions, G:C→T:A transversions, and 1-base deletions were the major mutations induced by 1,6-DNP as shown in Figure 2, which shows the mutant frequency in the treatment groups associated with each type of mutation. In the 1,6-DNP treated group, 47% of the mutations (36 out of 77 mutants) were

TABLE II. Classification of *gpt* Mutations From the Lungs of Control and 1,6-DNP-Treated Mice<sup>a</sup>

Type of mutation in the <i>gpt</i> gene	Control <sup>b</sup>				1,6-DNP total <sup>c</sup>				1,6-DNP (mg)				
	Total/independent		%/% independent		Total/independent		%/% independent		Total/independent		%/% independent		
Base substitution													
Transition													
G:C→A:T (CpG site)	10/10 (3/3)	45/48	36/27 (21/13)	47/43	13/7 (9/4)	46/39	13/12 (6/5)	46/46	10/8 (6/4)	48/42			
A:T→G:C	2/2	9/10	6/5	8/8	3/2	11/11	1/1	4/4	2/2	10/11			
Transversion													
G:C→T:A	4/4	18/19	13/11	17/17	6/4	21/22	5/5	18/19	2/2	10/11			
G:C→C:G	4/3	18/14	3/3	4/5	0	0	1/1	4/4	2/2	10/11			
A:T→T:A	0	0	1/1	1/2	1/1	4/6	0	0	0	0			
A:T→C:G	0	0	2/2	3/3	1/1	4/6	0	0	1/1	5/5			
Deletion													
1-base	2/2	9/10	13/12	17/19	2/2	7/11	7/6	25/23	4/4	19/21			
Insertion	0	0	3/2	4/3	2/1	7/6	1/1	4/4	0	0			
Total	22/21	100	77/63	100	28/18	100	28/26	100	21/19	100			

<sup>a</sup>Independent mutations were isolated no more than once from any individual mouse.

<sup>b</sup>Control mutations are the sum of the mutations obtained from control animals in this study plus the mutations obtained from control animals in a previous study [Hashimoto et al., 2005]. The numbers of each type of mutation in control animals from this study were obtained from Table III.

<sup>c</sup>Mutations combined from all treatment doses.

G:C→A:T transitions, while 17% (13/77) were G:C→T:A transversions together with an equal percentage of 1-base deletions. In control mice, 78% (7/9) of the total mutations were G:C→A:T transitions. To increase the number of control mutants used for comparison, 9 mutants from this study were combined with 13 control lung mutants isolated from a previous study performed analogously to this one [Hashimoto et al., 2005], and this pooled mutant spectrum is used for the data shown in Table II and the mutant frequency distribution shown in Figure 2. There were no significant differences between spectra of the 22 control mutations and 77 total 1,6-DNP-induced mutations (Table II) ( $P = 0.39$ , Adams-Skopek test).

The *gpt* mutations isolated from 1,6-DNP-treated mice are listed in Table III. Among the G:C→A:T transitions isolated from treated mice, five (at nucleotides 64, 110, 115, 116, and 418) were observed in four or more mice. These positions are therefore potential hotspots for 1,6-DNP mutations; however, no significant differences were observed between the positions of the control mutations isolated in this study and the positions of the 1,6-DNP mutations ( $P = 0.61$ , Adams-Skopek test). There were also no significant differences between the positions of the 22 control lung mutations pooled from this study and our previous study [Hashimoto et al., 2005] and the 77 1,6-DNP-induced mutations ( $P = 0.08$ , Adams-Skopek test). The predominant frameshift mutation after 1,6-DNP treatment was single base-pair deletions at G:C (9/13 = 69%). Seventy-seven percent of 1-base deletions (10/13) occurred in run sequences, and there were no hotspots for 1-base deletions.

DISCUSSION

DNPs are recognized as potent environmental mutagens. Moreover, 1,6-DNP is a carcinogen in experimental animals [Tokawa et al., 1984]. Using the Ames test, 43% of the direct mutagenicity of diesel particulate extracts was estimated to be due to contaminant DNPs [Nakagawa et al., 1983]. A 1,3-, 1,6-, and 1,8-DNP mixture was mutagenic in the liver, lung, colon, stomach, and bone marrow after intragastric injection in MutaMouse [Kohara et al., 2002]. However, little is known about the mechanism of in vivo mutagenesis by DNP.

To evaluate the mutagenicity of 1,6-DNP under exposure conditions appropriate for an air pollutant, the compound was administered intratracheally to *gpt*-delta mice. Treatment with 0–0.05 mg of this compound led to a linear increase in mutant and mutation frequency (Fig. 1), as shown previously with 0–2 mg B[a]P [Hashimoto et al., 2005]. The in vivo mutagenic potency (induced mutant frequency per amount of compound administered) for 1,6-DNP was  $32 \times 10^{-5}$  per mg, which was 13 times higher than that of B[a]P ( $2.4 \times 10^{-5}$  per mg) [Hashimoto et al., 2005], indicating that 1,6-DNP was a

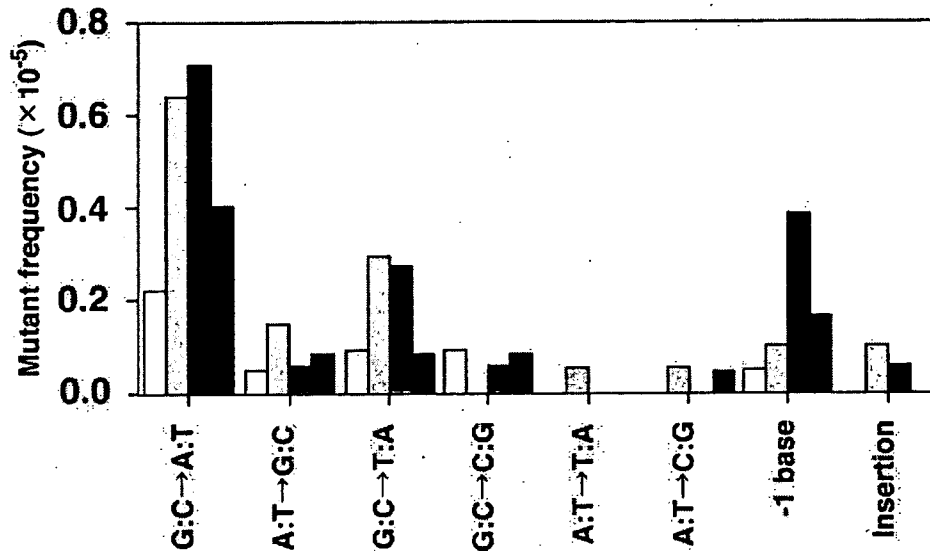


Fig. 2. Comparison of 1,6-DNP-induced and control mutation spectra in *gpt*-delta mice. White bar, control; light gray bar, 0.025 mg; dark gray bar, 0.05 mg; black bar, 0.1 mg. The analysis shown for control mutations is based on data combined from control animals in this study plus control animals from a previous study [Hashimoto et al., 2005].

more potent mutagen for the lung than B[a]P. However, the frequency was decreased at the highest dose (0.1 mg 1,6-DNP) to a lower level than that observed with 0.05 mg 1,6-DNP. We do not have any direct evidence to explain the decline in mutant frequency at high doses of 1,6-DNP in mice. Haugen et al. [1986] reported that unscheduled DNA synthesis, an index of excision repair in Clara cells and alveolar type-II cells, increased dose-dependently at low concentrations of 1,6-DNP, but decreased at high doses. This observation suggests that DNA adduct formation with 1,6-DNP is suppressed at high doses. Also, the amount of DNA adducts in 1,6-DNP-instilled rat lungs increased dose-dependently at low doses, but reached saturation at high doses [Smith et al., 1995]. The level of the 1,6-DNP-DNA adduct in lungs may be low at a dose of 0.1 mg 1,6-DNP, resulting in the lower mutant frequency. Finally it cannot be ruled out that cell proliferation in mice treated with 0.1 mg 1,6-DNP may not have been enough to fix the mutations because of the cytotoxicity of 1,6-DNP at high doses.

Our results indicate that G:C→A:T transitions, G:C→T:A transversions, and 1-base deletions are the major mutations induced by 1,6-DNP in the lung. On the other hand, Kohara et al. [2002] demonstrated that following the administration of DNP mixtures, the incidence of G:C→T:A transversions (43%) was higher than that of G:C→A:T transitions (22%) in the colon. Thus, the mutation spectrum of 1,6-DNP in the lung was different from the spectrum induced by the mixture of 1,3-, 1,6-, and 1,8-DNP in the colon. The metabolic reduction of 1,3-

DNP and 1-nitropyrene was reported to be less extensive than that of 1,6- or 1,8-DNP, suggesting that the reduction pathways are distinct between these nitro-PAHs [Djuric et al., 1986]. Reduction as well as *O*-acetylation are important in determining the extent of DNA binding by 1,6- and 1,8-DNP in vivo [IPCS, 2003]. 1,6- and 1,8-DNP form *N*-(deoxyguanosin-8-yl)-1-amino-6-nitropyrene (dG-C8-1-amino-6-NP) and *N*-(deoxyguanosin-8-yl)-1-amino-8-nitropyrene (dG-C8-1-amino-8-NP) adducts, respectively [Smith et al., 1995; IPCS, 2003], while the adducts of 1,3-DNP have not been determined. We propose that differences in DNA adduct formation contribute to the variations in mutant spectra between 1,6-DNP and the 1,3-, 1,6-, and 1,8-DNP mixture.

Smith et al. [1997] reported that 1,6-DNP-induced lung tumors contain mutated *K-ras*. Among 20 specimens, 5 mutations in *K-ras* codon 12 (4 GGT to TGT transversions and 1 GGT to GAT), and 9 mutations in *p53* exons 5–8 (8 substitutions at G:C base pairs and 1 deletion) were identified. These substitutions are consistent with the formation of dG adducts by 1,6-DNP. In our experiments, 1,6-DNP mainly induced substitutions in G:C pairs (61/77 = 79%), similar to the *K-ras* and *p53* mutations in lung tumors.

Interestingly, we showed in an earlier report that the predominant mutations in the lungs of Big Blue rats exposed to 6 mg/m<sup>3</sup> DE for 1 month were G:C→A:T and A:T→G:C transitions [Sato et al., 2000]. The major mutations identified in the lungs of *gpt*-delta mice following exposure to 3 mg/m<sup>3</sup> DE for 3 months were G:C→A:T transitions (unpublished results, Hashimoto



TABLE III. DNA Sequence Analysis of *gpt* Mutation Obtained From the Lung of Control and 1,6-DNP-Treated *gpt*-delta Mice

Type of mutation in the <i>gpt</i> gene	Nucleotide	Sequence change	Site	Amino acid change	Number		Number				
					Control all	1,6-DNP all	0.025 mg of 1,6-DNP	0.05 mg of 1,6-DNP	0.1 mg of 1,6-DNP		
Base substitution											
Transition											
G:C→A:T	26	tGg→tAg		Trp→Stop		1		1			
	64	Cga→Tga	CpG	Arg→Stop	1	5 <sup>a</sup>	1	2 <sup>b</sup>	2 <sup>b</sup>		
	92	gGc→gAc		Gly→Asp		1		1			
	110	cGt→cAt	CpG	Arg→His	1	12 <sup>c</sup>	6	3 <sup>b</sup>		3	
	115	Ggt→Agt	CpG	Gly→Ser		4 <sup>c</sup>	2 <sup>b</sup>	1		1	
	116	gGt→gAt		Gly→Asp		4 <sup>c</sup>	1	2 <sup>b</sup>		1	
	128	gGt→gAt		Gly→Asp	1						
	401	tGg→tAg		Trp→Stop	1	1				1	
	402	tgG→tgA		Trp→Stop		1				1	
	406	Gaa→Aaa		Glu→Lys		2 <sup>b</sup>		2 <sup>b</sup>			
	417	tgG→tgA		Trp→Stop	1						
	418	Gat→Aat		Asp→Asn	2 <sup>b</sup>	5 <sup>c</sup>	3 <sup>b</sup>	1		1	
	A:T→G:C	56	cTc→cCc		Leu→Pro		1				1
149		cTg→cCg		Leu→Pro		1	1				
275		gAt→gGt		Asp→Gly		2	2				
419		gAt→gGt		Asp→Gly		2 <sup>b</sup>		1		1	
Transversion											
G:C→T:A	59	gCa→gAa		Ala→Glu		1				1	
	115	Ggt→Tgt	CpG	Gly→Cys		1		1			
	140	gCg→gAg	CpG	Ala→Glu		1		1			
	244	Gaa→Taa	CpG	Glu→Stop	1						
	262	Gat→Tat		Asp→Tyr		2 <sup>b</sup>	2 <sup>b</sup>				
	287	aCt→aAt		Thr→Asn		3	3				
	402	tgG→tgT		Trp→Cys		1		1			
	406	Gaa→Taa		Glu→Stop		2 <sup>b</sup>	1	1			
	413	cCg→cAg	CpG	Pro→Gln		1				1	
	418	Gat→Tat		Asp→Tyr		1		1			
	G:C→C:G	131	gCg→gGg	CpG	Ala→Gly		1		1		
		206	cGc→cCc	CpG	Arg→Pro		1				1
		413	cCg→cGg	CpG	Pro→Arg		1				1
A:T→T:A	10	Aaa→Taa		Lys→Stop		1	1				
A:T→C:G	106	Agc→Cgc		Ser→Arg		1				1	
	254	aTc→aGc		Ile→Ser		1	1				
Deletion											
1-base	8-12	gAAAAAt→gAAAAAt				1		1			
	32	aTg→ag				1		1			
	97	tAt→tt				1				1	
	115-116	cGGt→cGt				1		1			
	126-128	cGGGt→cGGt				1		1			
	170-171	aCCg→aCg				1	1				
	237	gCg→gg				1				1	
	278-279	aCCg→aCg				1				1	
	315-318	cAAAAG→cAAAag				1	1				
	358-359	tCCg→tCg				2		2			
	416-418	tGGGa→tGGa				1	1	1			
	423-425	tGGGc→tGGc					1			1	
	Insertion										
	291	cg→cAg				2	2				
	255	cg→cGTTATTGATGACCTg				1		1			

<sup>a</sup>Mutation found in five different mice.<sup>b</sup>Mutation found in two different mice.<sup>c</sup>Mutation found in four different mice.

et al.). As observed in DE-exposed lungs, G:C→A:T transition was the major base substitution (47%, 36 out of 77 mutants) induced by 1,6-DNP (Fig. 2), while G:C→T:A transversions were the predominant base sub-

stitution in B[a]P-instilled lungs of *gpt*-delta mice [Hashimoto et al., 2005]. Our results provide useful information on the in vivo mutations induced by 1,6-DNP in the lung.

## ACKNOWLEDGMENTS

The authors thank Dr. Hiroaki Shiraishi, Dr. Michi Matsumoto, and Dr. Wakae Maruyama for support and advice.

## REFERENCES

- Adams WT, Skopek TR. 1987. Statistical test for the comparison of samples from mutational spectra. *J Mol Biol* 194:391-396.
- Brightwell J, Fouillet X, Cassano-Zoppi AL, Gatz R, Duchosal F. 1986. Neoplastic and functional changes in rodents after chronic inhalation of engine exhaust emissions. *Dev Toxicol Environ Sci* 13: 471-485.
- Cariello NF, Piegorsch WW, Adams WT, Skopek TR. 1994. Computer program for the analysis of mutational spectra: Application to *p53* mutations. *Carcinogenesis* 15:2281-2285.
- Delclos KB, Walker RP, Dooley KL, Fu PP, Kadlubar FF. 1987. Carcinogen-DNA adduct formation in the lungs and livers of preweanling CD-1 male mice following administration of [<sup>3</sup>H]-6-nitrochrysene, [<sup>3</sup>H]-6-aminochrysene, and [<sup>3</sup>H]-1,6-dinitropyrene. *Cancer Res* 47:6272-6277.
- Djuric Z, Potter DW, Heflich RH, Beland FA. 1986. Aerobic and anaerobic reduction of nitrated pyrenes in vitro. *Chem Biol Interact* 59:309-324.
- Harris JE. 1983. Diesel emission and lung cancer. *Risk Anal* 3:83-100.
- Hashimoto AH, Amanuma K, Hiyoshi K, Takano H, Masumura K, Nohmi T, Aoki Y. 2005. In vivo mutagenesis induced by benzo[a]pyrene instilled into the lung of *gpt* delta transgenic mice. *Environ Mol Mutagen* 45:365-373.
- Haugen A, Aune T, Deilhaug T. 1986. Nitropyrene-induced DNA repair in Clara cells and alveolar type-II cells isolated from rabbit lung. *Mutat Res* 175:259-262.
- IPCS (International Programme on Chemical Safety). 2003. Selected nitro- and nitro-oxy-polycyclic aromatic hydrocarbons. Environmental health criteria 229. Geneva:World Health Organization. pp 161-164.
- Iwagawa M, Maeda T, Izumi K, Otsuka H, Nishifuji K, Ohnishi Y, Aoki S. 1989. Comparative dose-response study on the pulmonary carcinogenicity of 1,6-dinitropyrene and benzo[a]pyrene in F344 rats. *Carcinogenesis* 10:1285-1290.
- Jeffrey AM, Santella RM, Wong D, Hsieh LL, Heisig V, Duskocil G, Ghayourmanesh S. 1990. Metabolic activation of nitropyrenes and diesel particulate extracts. *Res Rep Health Eff Inst* 34:1-30.
- Kohara A, Suzuki T, Honma M, Oomori T, Ohwada T, Hayashi M. 2002. Dinitropyrenes induce gene mutations in multiple organs of the lambda/lacZ transgenic mouse (Muta Mouse). *Mutat Res* 515:73-83.
- Masumura K, Matsui M, Katoh M, Horiya N, Ueda O, Tanabe H, Yamada M, Suzuki H, Sofuni T, Nohmi T. 1999. Spectra of *gpt* mutations in ethylnitrosourea-treated and untreated transgenic mice. *Environ Mol Mutagen* 34:1-8.
- Masumura K, Matsui K, Yamada M, Horiguchi M, Ishida K, Watanabe M, Wakabayashi K, Nohmi T. 2000. Characterization of mutations induced by 2-amino-1-methyl-6-phenylimidazo[4,5-b]pyridine in the colon of *gpt* delta transgenic mouse: Novel G:C deletions beside runs of identical bases. *Carcinogenesis* 21:2049-2056.
- Masumura K, Totsuka Y, Wakabayashi K, Nohmi T. 2003. Potent genotoxicity of aminophenylnorharman, formed from non-mutagenic norharman and aniline, in the liver of *gpt* delta transgenic mouse. *Carcinogenesis* 24:1985-1993.
- Mermelstein R, Kiriazides DK, Butler M, McCoy EC, Rosenkranz HS. 1981. The extraordinary mutagenicity of nitropyrenes in bacteria. *Mutat Res* 89:187-196.
- Muranaka M, Suzuki S, Koizumi K, Takafuji S, Miyamoto T, Ikemori R, Tokiwa H. 1986. Adjuvant activity of diesel-exhaust particulates for the production of IgE antibody in mice. *J Allergy Clin Immunol* 77:616-623.
- Nakagawa R, Kitamori S, Horikawa K, Nakashima K, Tokiwa H. 1983. Identification of dinitropyrenes in diesel-exhaust particles. Their probable presence as the major mutagens. *Mutat Res* 124:201-211.
- Nohmi T, Katoh M, Suzuki H, Matsui M, Yamada M, Watanabe M, Suzuki M, Horiya N, Ueda O, Shibuya T, Ikeda H, Sofuni T. 1996. A new transgenic mouse mutagenesis test system using Spi<sup>-</sup> and 6-thioguanine selections. *Environ Mol Mutagen* 28:465-470.
- Nohmi T, Suzuki T, Masumura K. 2000. Recent advances in the protocols of transgenic mouse mutation assays. *Mutat Res* 455:191-215.
- Rosenkranz HS, Mermelstein R. 1983. Mutagenicity and genotoxicity of nitroarenes. All nitro-containing chemicals were not created equal. *Mutat Res* 114:217-267.
- Salmeen IT, Pero AM, Zator R, Schuetzle D, Riley TL. 1984. Ames assay chromatograms and the identification of mutagens in diesel particle extracts. *Environ Sci Technol* 18:375-382.
- Sato H, Sone H, Sagai M, Suzuki KT, Aoki Y. 2000. Increase in mutation frequency in lung of Big Blue rat by exposure to diesel exhaust. *Carcinogenesis* 21:653-661.
- Smith BA, Fullerton NF, Heflich RH, Beland FA. 1995. DNA adduct formation and T-lymphocyte mutation induction in F344 rats implanted with tumorigenic doses of 1,6-dinitropyrene. *Cancer Res* 55:2316-2324.
- Smith BA, Manjanatha MG, Pogribny IP, Mittelstaedt RA, Chen T, Fullerton NF, Beland FA, Heflich RH. 1997. Analysis of mutations in the *K-ras* and *p53* genes of lung tumors and in the *hprt* gene of 6-thioguanine-resistant T-lymphocytes from rats treated with 1,6-dinitropyrene. *Mutat Res* 379:61-68.
- Sugimura T, Takayama S. 1983. Biological actions of nitroarenes in short-term tests on *Salmonella*, cultured mammalian cells and cultured human tracheal tissues: Possible basis for regulatory control. *Environ Health Perspect* 47:171-176.
- Suzuki T, Itoh S, Nakajima M, Hachiya N, Hara T. 1999. Target organ and time-course in the mutagenicity of five carcinogens in Muta-Mouse: A summary report of the second collaborative study of the transgenic mouse mutation assay by JEMS/MMS. *Mutat Res* 444:259-268.
- Takano H, Yanagisawa R, Ichinose T, Sadakane K, Inoue K, Yoshida S, Takeda K, Yoshino S, Yoshikawa T, Morita M. 2002. Lung expression of cytochrome P450 1A1 as a possible biomarker of exposure to diesel exhaust particles. *Arch Toxicol* 76:146-151.
- Takayama S, Ishikawa T, Nakajima H, Sato S. 1985. Lung carcinoma induction in Syrian golden hamsters by intratracheal instillation of 1,6-dinitropyrene. *Jpn J Cancer Res* 76:457-461.
- Thybaud V, Dean S, Nohmi T, de Boer J, Douglas GR, Glickman BW, Gorelick NJ, Heddle JA, Heflich RH, Lambert I, Martus HJ, Mirsalis JC, Suzuki T, Yajima N. 2003. In vivo transgenic mutation assays. *Mutat Res* 540:141-151.
- Tokiwa H, Otofujii T, Horikawa K, Kitamori S, Otsuka H, Manabe Y, Kinouchi T, Ohnishi Y. 1984. 1,6-Dinitropyrene: Mutagenicity in *Salmonella* and carcinogenicity in BALB/c mice. *J Natl Cancer Inst* 73:1359-1363.



## Combined genotoxic effects of radiation and a tobacco-specific nitrosamine in the lung of *gpt* delta transgenic mice

Megumi Ikeda<sup>a,b</sup>, Ken-ichi Masumura<sup>a</sup>, Yasuteru Sakamoto<sup>a</sup>, Bing Wang<sup>c</sup>,  
Mitsuru Neno<sup>c</sup>, Keiko Sakuma<sup>b</sup>, Isamu Hayata<sup>c</sup>, Takehiko Nohmi<sup>a,\*</sup>

<sup>a</sup> Division of Genetics and Mutagenesis, National Institute of Health Sciences, 1-18-1 Kamiyoga, Setagaya-ku, Tokyo 158-8501, Japan

<sup>b</sup> Graduate School of Nutrition and Health Sciences, Kagawa Nutrition University, 3-9-21 Chiyoda, Sakado-shi, Saitama 350-0288, Japan

<sup>c</sup> Radiation Effect Mechanisms Research Group, Research Center of Radiation Protection, National Institute of Radiological Sciences, 4-9-1 Anagawa, Inage-ku, Chiba-shi, Chiba 263-8555, Japan

Received 22 May 2006; received in revised form 25 July 2006; accepted 31 July 2006

Available online 7 September 2006

### Abstract

It is important to evaluate the health effects of low-dose-rate or low-dose radiation in combination with chemicals as humans are exposed to a variety of chemical agents. Here, we examined combined genotoxic effects of low-dose-rate radiation and 4-(methylnitrosamino)-1-(3-pyridyl)-1-butanone (NNK), the most carcinogenic tobacco-specific nitrosamine, in the lung of *gpt* delta transgenic mice. In this mouse model, base substitutions and deletions can be separately analyzed by *gpt* and *Spi*<sup>-</sup> selections, respectively. Female *gpt* delta mice were either treated with  $\gamma$ -irradiation alone at a dose rate of 0.5, 1.0 or 1.5 mGy/h for 22 h/day for 31 days or combined with NNK treatments at a dose of 2 mg/mouse/day, i.p. for four consecutive days in the middle course of irradiation. In the *gpt* selection, the NNK treatments enhanced the mutation frequencies (MFs) significantly, but no obvious combined effects of  $\gamma$ -irradiation were observable at any given radiation dose. In contrast, NNK treatments appeared to suppress the *Spi*<sup>-</sup> large deletions. In the *Spi*<sup>-</sup> selection, the MFs of deletions more than 1 kb in size increased in a dose-dependent manner. When NNK treatments were combined, the dose–response curve became bell-shaped where the MF at the highest radiation dose decreased substantially. These results suggest that NNK treatments may elicit an adaptive response that eliminates cells bearing radiation-induced double-strand breaks in DNA. Possible mechanisms underlying the combined genotoxicity of radiation and NNK are discussed, and the importance of evaluation of combined genotoxicity of more than one agent is emphasized.

© 2006 Elsevier B.V. All rights reserved.

**Keywords:** Combined genotoxic effects; Radiation; NNK; Lung cancer; *gpt* delta mice; Deletion

### 1. Introduction

Environmental factors play important roles in the etiology of human cancer [1]. Of various environmental hazardous compounds, cigarette smoke is the

most causative factor associated with the increase in cancer risk in humans. Tobacco smoking plays a major role in the etiology of lung, oral cavity and esophageal cancers, and a variety of chronic degenerative diseases [2]. Although cigarette smoke is a mixture of about 4000 chemicals including more than 60 known human carcinogens, 4-(methylnitrosamino)-1-(3-pyridyl)-1-butanone (nicotine-derived nitrosamino ketone, NNK) is the most carcinogenic tobacco-specific nitrosamine [3,4]. NNK induces lung tumors in mice,

\* Corresponding author. Tel.: +81 3 3700 9873;  
fax: +81 3 3707 6950.

E-mail address: [nohmi@nihs.go.jp](mailto:nohmi@nihs.go.jp) (T. Nohmi).

rats and hamsters, and International Agency for Research on Cancer has concluded that exposure to NNK and NNN (*N*'-nitrosornicotine) is carcinogenic to humans [5]. NNK is metabolically activated by CYP (P-450) enzymes in the lung and generates *O*<sup>6</sup>-methylguanine in DNA, which leads to G:C to A:T mutations, and the subsequent activation of *Ki-ras* proto-oncogene, an initiation of tumor development [6,7].

Radiation, on the other hand, is one of the most causative physical factors that induce human cancer. Radiation induces double-strand breaks (DSBs) in DNA, which lead to chromosome aberrations and cell deaths, and generates a variety of oxidative DNA damage [8]. Because of the genotoxicity, radiation at high doses clearly induces various tumors in humans [9]. Even at low doses, residential exposure to radioactive radon and its decay products may account for about 10% of all lung cancer deaths in the United States and about 20% of the lung cancer cases in Sweden [10,11].

Since humans are exposed to a variety of chemical and physical agents that may induce cancer, these factors may interact with each other and the action of one agent may be influenced by exposure to another agent [12]. The risk from combined exposure to more than one agent may be substantially higher or lower than predicted from the sum of the individual agents. In fact, low-dose radiation can induce an adaptive response, causing rodent or human cells to become resistant to genotoxic damage by subsequent higher doses of radiation [13]. Pre-exposure to alkylating agents at low doses induces another adaptive response that provides mechanisms by which the exposed bacterial cells can tolerate the higher challenging doses of genotoxic agents [14]. In addition, mitomycin C, bleomycin, hydrogen peroxide, metals and quercetin may also induce an adaptive response [15].

To explore the mechanisms underlying the interactive effects of chemical and physical agents on carcinogenesis, we examined the combined genotoxic effects of NNK and  $\gamma$ -irradiation in the lung of *gpt* delta transgenic mice [16]. In this mouse model, point mutations and deletions are separately analyzable by *gpt* and *Spi*<sup>-</sup> selections, respectively [17]. Point mutations such as base substitutions are induced by a number of chemical carcinogens including NNK [18]. *Spi*<sup>-</sup> selection detects deletions in size between 1 bp and 10 kb [19]. Deletions in size more than 1 kb, which we call large deletions in this study, are efficiently induced by  $\gamma$ -ray, X-ray and carbon-ion irradiation [20], and are thought to be generated by non-homologous end joining (NHEJ) of DSBs in DNA [21].

We report here that low-dose-rate  $\gamma$ -irradiation enhanced the mutation frequencies (MFs) of the large

deletions in the lung of *gpt* delta mice in a dose-dependent manner. When combined with NNK treatments, however, the MF at the highest radiation dose, i.e., 1.02 Gy, was reduced by more than 50%, suggesting that NNK treatments may induce an adaptive response against radiation-induced deletion mutations. We discuss possible mechanisms of the adaptive response and emphasize the importance of the risk assessment of combined genotoxic effects of radiation and chemicals in vivo.

## 2. Materials and methods

### 2.1. Treatment of mice

*gpt* delta C57BL/6J transgenic mice were maintained in the conventional animal facility of National Institute of Radiological Sciences, Chiba, Japan, according to the institutional animal care guidelines. They were housed in autoclaved aluminum cages with sterile wood chips for bedding and given free access to standard laboratory chow (MB-1, Funabashi Farm Co., Japan) and acidified water under controlled lighting (12 h light/dark cycle). Seven-week-old female *gpt* delta mice were divided to eight groups each consisting of six mice. Three groups were  $\gamma$ -irradiated at a dose rate of 0.5, 1.0 or 1.5 mGy/h for 22 h/day for 2 weeks (Fig. 1). After the irradiation, three groups of mice were treated with a single i.p. injection of NNK (Toronto Research Chemicals, Toronto, Canada) dissolved in saline at a daily dose of 2 mg/mouse for four consecutive days. The irradiation continued during the 4-day treatments, and the mice were kept in the cage for another 2 weeks with irradiation. Three control groups were  $\gamma$ -irradiated as described but received saline instead of NNK. The whole irradiation period was 31 days, and the total estimated doses were 0.34, 0.68 and 1.02 Gy, respectively. Another control group of mice was treated with NNK as described but without  $\gamma$ -irradiation. The third control was kept in the cage for 31 days without  $\gamma$ -irradiation or NNK treatments. The source of radiation was <sup>137</sup>Cs, and the dose rate was estimated by a fluorescent glass dosimeter. The non-irradiated control groups were placed behind a concrete wall of 1 m thickness. The mice were sacrificed by cervical vertebral dislocation. The liver and lung were removed, placed immediately in liquid nitrogen, and stored at -80 °C until analysis.

### 2.2. DNA isolation and in vitro packaging of DNA

High-molecular-weight genomic DNA was extracted from the lung and the liver using the RecoverEase DNA Isolation Kit (Stratagene, La Jolla, CA). Lambda EG10 phages were rescued using Transpack Packaging Extract (Stratagene, La Jolla, CA).

### 2.3. *gpt* mutation assay

The *gpt* mutagenesis assay was performed according to previously described methods [17]. Briefly, *Escherichia coli*

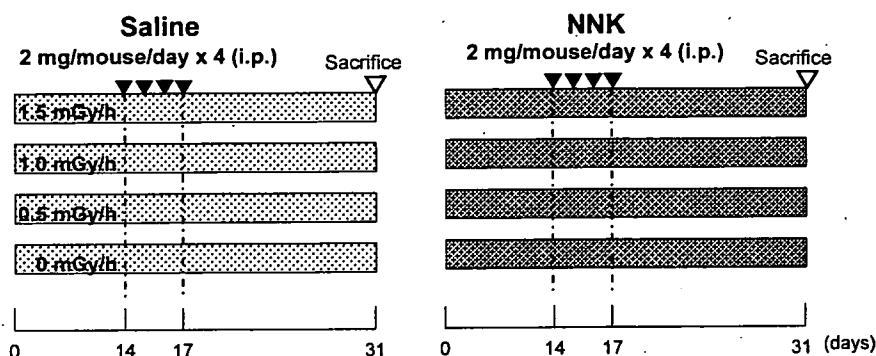


Fig. 1. An experimental design to examine the combined genotoxicity of  $\gamma$ -irradiation and NNK treatments in the lung of mice. Female 7-week-old *gpt* delta mice were divided into eight groups each composed of six mice. Three groups of mice were irradiated at a dose rate of 0.5, 1.0 or 1.5 mGy/h for 22 h/day for 14 days and treated with NNK at a daily dose of 2 mg/mouse for four consecutive days. The irradiation continued during the NNK treatments and the following 14 days before sacrifice. The total radiation doses were 0.34, 0.68 and 1.02 Gy, respectively. Control three groups of mice were  $\gamma$ -irradiated but without NNK treatments. Another control group was treated with NNK but without  $\gamma$ -irradiation. The third control was kept in the cage for 31 days without  $\gamma$ -irradiation or NNK treatments. Transgene  $\lambda$ EG10 DNA was rescued from the lung of mice, and the base substitutions and deletions were analyzed by *gpt* and *Spi*<sup>-</sup> selection, respectively.

YG6020 expressing Cre recombinase was infected with the rescued phage. The bacteria were then spread onto M9 salts plates containing chloramphenicol (Cm) and 6-thioguanin (6-TG), and incubated for 72 h at 37 °C for selection for the colonies harboring a plasmid carrying the Cm acetyltransferase (*cat*) gene and a mutated *gpt* gene. The 6-TG-resistant colonies were streaked again onto the same selection plates for confirmation of the resistant phenotype. All the confirmed *gpt* mutants recovered from the lung were sequenced and the identical mutations from the same mouse counted one mutant. The *gpt* MFs in the lung were calculated by dividing the number of the *gpt* mutants after sequencing by the number of rescued plasmids, which was estimated from the number of colonies on plates containing Cm but without 6-TG. Since no *gpt* mutants recovered from the liver were sequenced, the MFs in the liver were calculated by dividing the number of confirmed 6-TG-resistant colonies by the number of rescued plasmids.

#### 2.4. PCR and DNA sequencing analysis of 6-TG-resistant mutants

A 739 bp DNA fragment containing the *gpt* gene was amplified by polymerase chain reaction (PCR) using primers 1 and 2 [17]. The reaction mixture contained 5 pmol of each primer and 200 mM of each dNTP. PCR amplification was carried out using Ex Taq DNA polymerase (Takara Bio, Shiga, Japan) and performed with a Model PTC-200 Thermal Cycler (MJ Research, Waltham, MA). PCR products were analyzed by agarose gel electrophoresis to determine the amount of the products. DNA sequencing of the *gpt* gene was performed with BigDye™ Terminator Cycle Sequencing Kit (Applied Biosystems, Foster City, CA) using sequencing primer *gptA2* (5'-TCTCGCGCAACCTATTTTCCC-3'). The sequencing reaction products were analyzed on an Applied Biosystems model 310 genetic analyzer (Applied Biosystems, Foster City, CA).

#### 2.5. *Spi*<sup>-</sup> mutation assay

The *Spi*<sup>-</sup> assay was performed as described previously [17]. The lysates of *Spi*<sup>-</sup> mutants were obtained by infection of *E. coli* LE392 with the recovered *Spi*<sup>-</sup> mutants. The lysates were used as templates for PCR analysis to determine the deleted regions. Sequence changes in the *gam* and *redAB* genes, and the outside of the *gam/redAB* genes were identified by DNA sequencing analysis [22]. The appropriate primers for DNA sequencing were selected based on the results of PCR analysis. The entire sequence of  $\lambda$ EG10 is available at <http://dgm2alpha.nhis.go.jp>.

#### 2.6. Statistical analysis

All data are expressed as mean  $\pm$  standard deviations of the MFs of six mice for lung and those of four mice for liver. Differences between groups were tested for statistical significance using a Student's *t*-test. A *p* value less than 0.05 denoted the presence of a statistically significant difference.

### 3. Result

#### 3.1. *gpt* MFs in the lung of NNK-treated and $\gamma$ -irradiated *gpt* delta mice

We measured the *gpt* MFs in the lung of *gpt* delta mice untreated or treated with NNK in the absence or the presence of  $\gamma$ -irradiation (Fig. 2). NNK treatments significantly enhanced the MFs over the control groups. The mean MFs ( $\times 10^{-6}$ ) of NNK-treated versus saline-treated groups were  $14.3 \pm 6.9$  versus  $4.2 \pm 4.0$ ,  $20.7 \pm 5.1$  versus  $4.7 \pm 3.0$ ,  $15.2 \pm 7.3$  versus  $2.0 \pm 2.1$  and  $17.2 \pm 7.9$  versus  $2.7 \pm 1.4$  at the dose rates of 0, 0.5, 1.0 and 1.5 mGy/h, respectively. The  $\gamma$ -irradiation

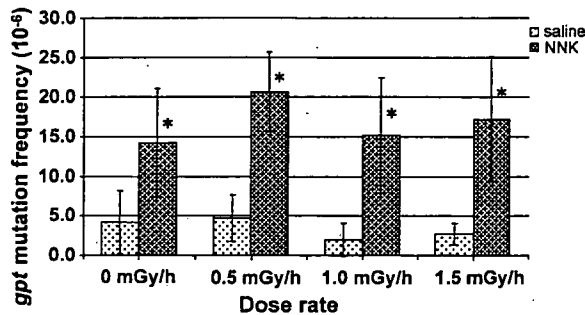


Fig. 2. *gpt* MFs in the lung of mice untreated or treated with NNK in the absence or the presence of  $\gamma$ -irradiation. An asterisk (\*) denotes  $p < 0.05$  ( $n = 6$ ) in a Student's *t*-test of MF of NNK-treated vs. the corresponding untreated mice. Vertical bars show the standard deviations with mice as the unit of comparison.

alone, i.e., the saline-treated group, did not enhance the *gpt* MF under the conditions. Hence, the increases in MFs are due to NNK treatments. Although the individual MFs slightly varied, there was no significant difference among the four MFs of the NNK-treated groups. Thus, we suggested that the irradiation did not modify the genotoxicity of NNK in the lung of mice.

To confirm the results in the lung, we analyzed the *gpt* MFs in the liver of the NNK-treated and saline-treated groups. The mean MFs ( $\times 10^{-6}$ ) of NNK-treated versus saline-treated groups were  $134 \pm 48$  versus  $8.1 \pm 3.8$ ,  $105 \pm 31$  versus  $8.7 \pm 3.5$ ,  $101 \pm 18$  versus  $8.0 \pm 4.2$  and  $128 \pm 76$  versus  $6.8 \pm 0.6$  at the dose rates of 0, 0.5, 1.0 and 1.5 mGy/h, respectively. Although NNK treatments induced mutations much more strongly in the liver than in the lung, there were no significant modulating effects of radiation on the NNK-induced mutations in the liver.

The irradiation might modulate specific types of mutations without affecting the total *gpt* MFs. To exam-

ine the possibility, we determined the mutation spectra of the *gpt* gene in the lung and examined whether the radiation affected specific types of mutations (Table 1). NNK treatments induced G:C to A:T, G:C to T:A, A:T to T:A and A:T to C:G mutations. In particular, A:T to T:A mutations were induced more than 20-fold by NNK treatments. We observed, however, no remarkable variations of mutation spectra associated with the dose rates of combined radiation. Thus, we concluded that the irradiation did not enhance or suppress the base substitutions induced by NNK in the lung of *gpt* delta mice significantly.

### 3.2. *Spi*<sup>-</sup> MFs in the lung of NNK-treated and $\gamma$ -irradiated *gpt* delta mice

Next, we measured the *Spi*<sup>-</sup> MFs in the lung of *gpt* delta mice untreated or treated with NNK in the absence or the presence of  $\gamma$ -irradiation. The mean *Spi*<sup>-</sup> MFs ( $\times 10^{-6}$ ) of NNK-treated versus saline-treated groups were  $5.15 \pm 2.34$  versus  $4.11 \pm 0.98$ ,  $5.47 \pm 1.98$  versus  $5.06 \pm 3.50$ ,  $5.36 \pm 1.56$  versus  $4.09 \pm 0.80$  and  $5.39 \pm 2.56$  versus  $4.65 \pm 1.78$  at the dose rates of 0, 0.5, 1.0 and 1.5 mGy/h, respectively. These results suggest that neither NNK treatments nor the irradiation enhanced the *Spi*<sup>-</sup> MFs in the lung significantly.

To investigate the combined effects of NNK and  $\gamma$ -irradiation on specific types of deletion mutations, we identified all the *Spi*<sup>-</sup> mutations by DNA sequencing analysis (Table 2). Of various classes of deletions observed, only the MFs of large deletions in the size of more than 1 kb increased in a dose-dependent manner in the saline-treated group. To examine the dose-response in more detail, we determined the MFs of the large deletions

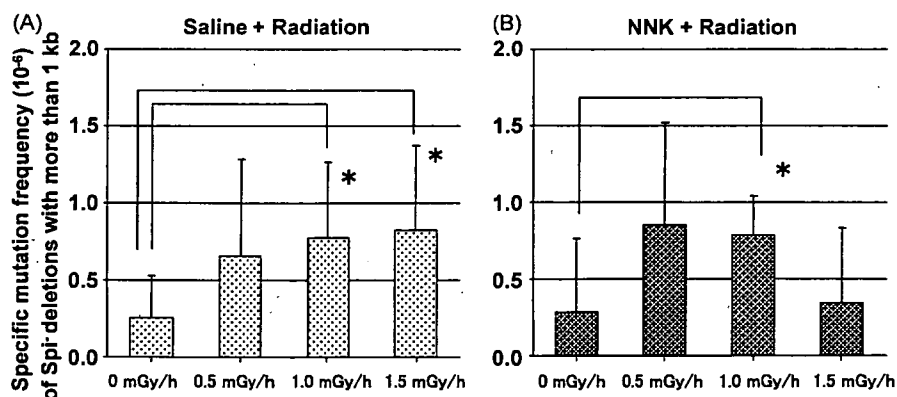


Fig. 3. Specific MF of large deletions with the size of more than 1 kb in the lung of unirradiated or  $\gamma$ -irradiated mice. The mice were not treated (A) or treated with NNK (B). An asterisk (\*) denotes  $p < 0.05$  ( $n = 5$ ) in a Student's *t*-test of MF of  $\gamma$ -irradiated vs. the corresponding unirradiated mice. Vertical bars show the standard deviations with mice as the unit of comparison.

Table 1  
*gpt* mutation spectra in the lung of NNK-treated and  $\gamma$ -irradiated *gpt* delta mice

Treatment: saline	0 mGy/h			0.5 mGy/h			1.0 mGy/h			1.5 mGy/h		
	No.	MF ( $\times 10^{-6}$ )	%	No.	MF ( $\times 10^{-6}$ )	%	No.	MF ( $\times 10^{-6}$ )	%	No.	MF ( $\times 10^{-6}$ )	%
Base substitution												
Transition												
G:C $\rightarrow$ A:T	15(6)	1.81	43	12(6)	1.76	38	5(2)	0.61	29	8(4)	0.81	30
A:T $\rightarrow$ G:C	2	0.24	6	4	0.59	13	1	0.12	6	2	0.20	7
Transversion												
G:C $\rightarrow$ T:A	1	0.12	3	5(2)	0.73	16	1	0.12	6	6(1)	0.61	22
G:C $\rightarrow$ C:G	1	0.12	3	0	0.00	0	0	0.00	0	2(2)	0.20	7
A:T $\rightarrow$ T:A	1	0.12	3	1	0.15	3	1	0.12	6	1	0.10	4
A:T $\rightarrow$ C:G	3	0.36	9	1	0.15	3	1	0.12	6	1	0.10	4
Deletion												
-1 bp	8	0.97	23	6	0.88	19	7	0.85	41	6	0.61	22
>2 bp	3			2			5			3		
	5			4			2			3		
Insertion												
	3	0.36	9	3	0.44	9	1	0.12	6	1	0.10	4
Others												
	1	0.12	3	0	0.00	0	0	0.00	0	0	0.00	0
	35	4.23	100	32	4.69	100	17	2.06	100	27	2.73	100
Treatment: NNK												
	0 mGy/h			0.5 mGy/h			1.0 mGy/h			1.5 mGy/h		
	No.	MF ( $\times 10^{-6}$ )	%	No.	MF ( $\times 10^{-6}$ )	%	No.	MF ( $\times 10^{-6}$ )	%	No.	MF ( $\times 10^{-6}$ )	%
Base substitution												
Transition												
G:C $\rightarrow$ A:T	24(2)	5.11	36	45(8)	8.02	39	32(5)	5.85	39	54(6)	8.51	50
A:T $\rightarrow$ G:C	0	0.00	0	7	1.25	6	6	1.10	7	2	0.32	2
Transversion												
G:C $\rightarrow$ T:A	9(2)	1.92	13	10(1)	1.78	9	7(1)	1.28	8	7(1)	1.10	6
G:C $\rightarrow$ C:G	0	0.00	0	2	0.36	2	0	0.00	0	3	0.47	3
A:T $\rightarrow$ T:A	13	2.77	19	26	4.64	22	17	3.11	21	17(1)	2.68	16
A:T $\rightarrow$ C:G	15	3.19	22	12	2.14	10	8	1.46	10	12(1)	1.89	11
Deletion												
-1 bp	5	1.06	8	12	2.14	10	9	1.65	11	12	1.89	11
>2 bp	5			6			4			5		
	0			6			5			7		
Insertion												
	1	0.21	2	0	0.00	0	4	0.73	5	1	0.16	1
Others												
	0	0.00	0	2	0.36	2	0	0.00	0	1	0.16	1
	67	14.26	100	116	20.68	100	83	15.18	100	109	17.18	100

No. stands for the number of mutations.

of each mouse and calculated the mean MF and standard derivations. The mean MFs ( $\times 10^{-6}$ ) and standard derivations were  $0.25 \pm 0.28$ ,  $0.66 \pm 0.63$ ,  $0.77 \pm 0.49$  and  $0.82 \pm 0.55$  at the dose rates of 0, 0.5, 1.0 and 1.5 mGy/h, respectively (Fig. 3A). The values at 1.0 and 1.5 mGy/h were about three-fold higher than the value at 0 mGy/h, and the differences were statistically

significant ( $p=0.04$ ). In contrast, the dose-response curve of large deletions in NNK-treated group was a bell shaped (Fig. 3B). The mean MFs ( $\times 10^{-6}$ ) and standard derivations of large deletions in the NNK-treated group were  $0.29 \pm 0.47$ ,  $0.85 \pm 0.66$ ,  $0.78 \pm 0.26$  and  $0.35 \pm 0.48$  at the dose rates of 0, 0.5, 1.0 and 1.5 mGy/h, respectively. It should be noted that the

Table 2  
Spi<sup>-</sup> mutation spectra in the lung of NNK-treated and  $\gamma$ -irradiated *gpt* delta mice

Treatment: saline	0 mGy/h			0.5 mGy/h			1.0 mGy/h			1.5 mGy/h		
	No.	MF ( $\times 10^{-6}$ )	%	No.	MF ( $\times 10^{-6}$ )	%	No.	MF ( $\times 10^{-6}$ )	%	No.	MF ( $\times 10^{-6}$ )	%
<b>1 bp deletion</b>												
<b>Simple</b>												
Guanine	9	0.49	12	7	0.59	12	5	0.34	8	4	0.30	7
Adenine	4	0.22	5	0	0.00	0	2	0.14	3	1	0.08	2
<b>In run</b>												
Guanine	13	0.71	17	15	1.27	25	12	0.82	20	13	0.99	21
Adenine	31	1.70	41	19	1.60	32	22	1.50	37	25	1.91	41
With b.s.	0	0.00	0	0	0.00	0	0	0.00	0	0	0.00	0
>2 bp deletion	15	0.82	20	17	1.43	28	17	1.16	28	13	0.99	21
2 bp ~ 1 kb	2	0.11	3	7	0.59	12	3	0.20	5	1	0.08	2
>1 kb	5	0.27	7	7	0.59	12	11	0.75	18	10	0.76	16
Complex	8	0.44	11	3	0.25	5	3	0.20	5	2	0.15	3
<b>Insertion</b>												
	3	0.16	4	2	0.17	3	2	0.14	2	5	0.38	8
	75	4.11	100	60	5.06	100	60	4.09	100	61	4.65	100
<b>Treatment: NNK</b>												
<b>0 mGy/h</b>												
	No.	MF ( $\times 10^{-6}$ )	%	No.	MF ( $\times 10^{-6}$ )	%	No.	MF ( $\times 10^{-6}$ )	%	No.	MF ( $\times 10^{-6}$ )	%
<b>1 bp deletion</b>												
<b>Simple</b>												
Guanine	5	0.61	12	4	0.46	8	4	0.50	9	4	0.48	9
Adenine	3	0.37	7	0	0.00	0	4	0.50	9	1	0.12	2
<b>In run</b>												
Guanine	9	1.10	21	19	2.17	40	9	1.12	21	14	1.68	31
Adenine	12	1.47	29	10	1.14	21	9	1.12	21	15	1.80	33
With b.s.	0	0.00	0	0	0.00	0	2	0.25	5	0	0.00	0
>2 bp deletion	12	1.47	29	10	1.14	21	11	1.37	26	11	1.32	24
2 bp ~ 1 kb	6	0.74	14	2	0.23	4	3	0.37	7	7	0.84	16
>1 kb	2	0.25	5	7	0.80	15	7	0.87	16	2	0.24	4
Complex	4	0.49	10	1	0.11	2	1	0.12	2	2	0.24	4
<b>Insertion</b>												
	1	0.12	2	5	0.57	10	4	0.50	9	0	0.00	0
	42	5.15	100	48	5.47	100	43	5.36	100	45	5.39	100

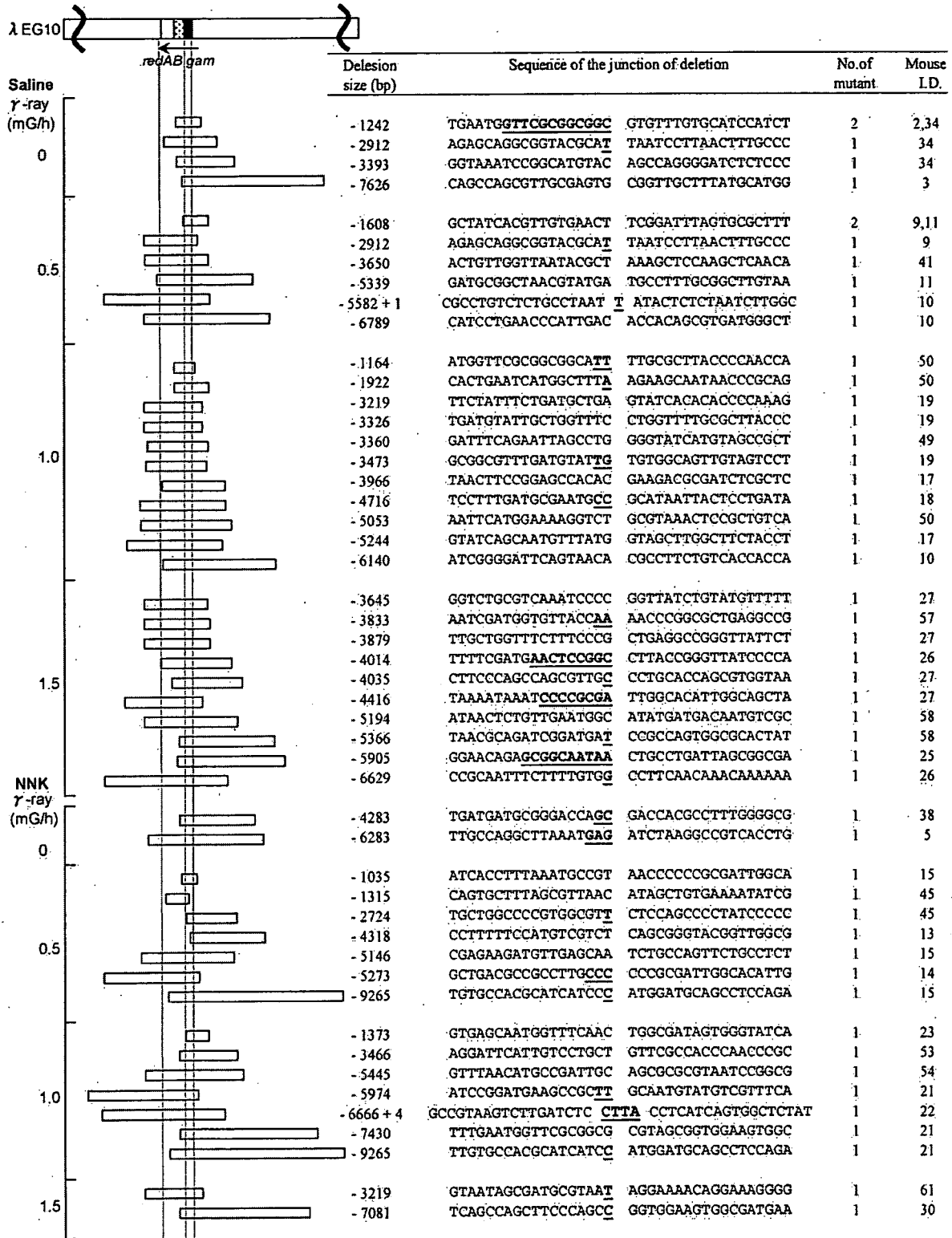
No. stands for the number of mutations. Specific MFs of large deletions more than 1 kb in size are italicised.

MF at 1.0 mGy/h ( $0.78 \times 10^{-6}$ ) was about three-fold higher than that of 0 mGy/h ( $p=0.04$ ) but the MF at 1.5 mGy/h ( $0.35 \times 10^{-6}$ ) was very similar to that of 0 mGy/h ( $0.29 \times 10^{-6}$ ). The  $p$  values of the differences

of MFs between saline-treated and NNK-treated groups at dose rates of 0, 0.5, 1.0 and 1.5 mGy/h were 0.44, 0.32, 0.48 and 0.09, respectively. From the results, we suggested that NNK treatments suppressed the induc-

Fig. 4. Molecular nature of large deletions recovered from the lung of *gpt* delta mice untreated or treated with NNK in the absence or the presence of  $\gamma$ -irradiation. Horizontal bars represent the deleted regions of mutants. Most of the mutants lack the entire *gam* gene and part of the *redAB* genes, but some lack the *gam* gene and the upstream region. The *gam* and *redAB* genes make an operon and the transcription starts from the upstream of the *gam* gene. Short homologous sequences in the junctions of the mutants are underlined. Underlined sequences, i.e., T or CTTA, in the middle of two sequences are inserted sequences in the junctions.





tion of large deletions at a dose rate of 1.5 mGy/h of  $\gamma$ -irradiation.

To further characterize the large deletions induced by the irradiation, we identified the size and junctions of all the 51 deletion mutants (Fig. 4). The size of deletions distributed from 1035 to 9265 bp. About half of the mutants had short homologous sequences up to 11 bp in the junctions while another half had no such short homologous sequences. Two mutants had 1 or 4 bp insertions in the junctions. There was no hot spot of the junctions so that only 2 out of 51 deletions were identified in two mice. There were no obvious differences between large deletions induced by radiation alone and those induced by radiation plus NNK treatments. These results suggest that radiation-induced DSBs in DNA caused large deletions either in the absence or the presence of NNK treatments.

#### 4. Discussion

Humans are exposed to a variety of exogenous and endogenous genotoxic agents. Thus, biological effects of radiation at low doses or low-dose-rate should be evaluated in combination with chemical exposure [12]. In fact, survey of chromosome aberrations in habitats in high-background radiation area in China indicates that cigarette smoking has stronger effects on induction of chromosome aberrations than has the elevated level of natural radiation [23]. Epidemiological studies on underground mineworkers exposed to high levels of radon or plutonium suggest the complexity of interactions between radiation and cigarette smoke in induction of lung tumors [24,25]. Hence, it is important to understand the fundamental mechanisms underlying the interactive genotoxicity and carcinogenicity of cigarette smoking and radiation for the risk assessment on human health.

To elucidate the mechanisms involved, we examined the combined genotoxicity of low-dose-rate  $\gamma$ -irradiation and a tobacco-specific nitrosamine NNK in the lung of *gpt* delta mice. In this study, we focused on whether  $\gamma$ -irradiation would modulate NNK-induced base substitutions and whether NNK treatments would modulate radiation-induced deletions. The mice were irradiated at dose rates of 0.5, 1.0 and 1.5 mGy/h for 22 h for 2 weeks and treated with NNK, i.e., 2 mg/mouse/day for four consecutive days, with irradiation (Fig. 1). The mice were irradiated at the same dose rates for another 2 weeks before sacrifice. Base substitutions and deletions in the lung detected by *gpt* and *Spi*<sup>-</sup> selection, respectively, were analyzed at the molecular levels. We chose the dose rates, i.e., 0.5, 1.0 and 1.5 mGy/h of  $\gamma$ -ray,

since Sakai et al. [26] report the suppression of carcinogenicity of 3-methylchroranthrene in ICR female mice by chronic low-dose-rate irradiation of  $\gamma$ -ray at 0.95 mGy/h. According to the report, there is an optimum dose rate of about 1 mGy/h to observe the suppressive effects, and the higher or lower dose rates fail to suppress the tumor induction.

In the present study, NNK treatments significantly enhanced the *gpt* MF (Fig. 2). We observed, however, no modulating effects, i.e., enhancement or suppression, of  $\gamma$ -irradiation at any given dose rate, on the NNK-induced mutations (Fig. 2). This conclusion holds true even when we analyzed the detailed mutation spectra (Table 1). NNK treatments induced similar pattern of base substitutions, i.e., G:C to A:T, G:C to T:A, A:T to T:A and A:T to C:G regardless of the dose rates of combined radiation. In contrast, we observed a suppressive effect of NNK treatments on the radiation-induced deletions.  $\gamma$ -Irradiation enhanced the MF of large deletions in the size of more than 1 kb in a dose-dependent manner (Fig. 3A and Table 2). When combined with NNK treatments, however, the dose–response curve became bell-shaped and the MF at the highest dose rate, i.e., 1.5 mGy/h, was reduced by more than 50% (Fig. 3B and Table 2). The total radiation dose at the highest dose rate was 1.02 Gy. The size of the large deletions was between about 1 and 9 kb, and about half of the large deletions had short homologous sequences in the junctions while other did not (Fig. 4). These features are similar to those of large deletions induced by high dose irradiation with heavy ion, X-ray and  $\gamma$ -ray [20]. Thus, we suggest that NNK induced an adaptive response that eliminated the cells bearing radiation-induced DSBs in DNA.

Previous studies show that low-dose radiation can induce an adaptive response, which causes cells to become resistant to damage by subsequent high doses of radiation [13,27]. Although the exact mechanisms of the adaptive response are not well understood, it is assumed that some proteins are induced by low-dose radiation and they recognize and remove the cells bearing DSB in DNA. Tucker et al. [28] report that the frequency of *Dlb-1* mutations in the small intestine in female F1 mice obtained by crossing SWR/J and C57BL/6 increases along with the total radiation doses of  $\gamma$ -ray, but it saturates and slightly decreases at high doses, i.e., 2–3 Gy (55 mGy/day  $\times$  42 or 63 days). Interestingly, our results also suggest that the MFs of the large deletions saturated slightly at the highest dose of 1.02 Gy (Fig. 3A). Thus the adaptive response might be induced slightly at the highest radiation dose even without NNK treatments. Nevertheless, concomitant NNK treatments much clearly suppressed the occurrence of large dele-

tions at the highest radiation dose. We speculate that NNK treatments plus radiation at the highest dose may induce p53-dependent apoptosis, which eliminates the cells bearing radiation-induced DSBs in DNA [29]. The involvement of p53 in the maintenance of genome stability is associated with several pathways such as cell cycle arrest, apoptosis and DNA repair. Low levels of DNA damage appear to enhance p53-dependent DNA repair while high levels induce apoptosis [30]. We envisage that NNK treatments plus radiation at the highest dose introduce genotoxic damage to the cells, the levels of which are enough to trigger the apoptosis. Zhou et al. [31] examined the combined effects of NNK and  $\alpha$ -particle irradiation with human–hamster hybrid cultured cells and concluded that the induction of chromosome deletions were additive when the NNK dose was low but a suppressive effect was observed at a higher NNK concentration. In vivo studies also suggest that exposure to high levels of cigarette smoke decrease the risk of lung cancer induced by radon in dogs [32]. However, a multiplicative effect of smoking and radon is observed in rats [33]. In humans, the definitive interaction models have not been established between smoking and radiation exposure [24,25]. Thus, further work is needed to clearly establish the interactive genotoxic mechanisms between radiation and cigarette smoking in vivo.

NNK, a tobacco-specific nitrosamine, is metabolically activated by  $\alpha$ -hydroxylation of the methyl and methylene groups [34]. Methylene hydroxylation leads to DNA methylation while methyl hydroxylation leads to pyridyloxobutylated DNA [35]. DNA methylation occurs at N7 and O<sup>6</sup> of guanine and O<sup>4</sup> and O<sup>2</sup> of thymine. It is suggested that O<sup>6</sup>-methylguanine (O<sup>6</sup>-mG) and pyridyloxobutylated DNA are responsible for G:C to A:T and G:C to T:A mutations, respectively, which activate Ki-ras oncogene in the mouse lung tumors induced by NNK [6]. In the present study, G:C to A:T and G:C to T:A mutations were induced by NNK treatments significantly (Table 1). Tiano et al. [36] examined the genotoxicity of NNK in AS52 hamster cells expressing human CYP2A6 and analyzed the induced mutations with the *gpt* gene as a reporter gene for mutations. Because of the lack of O<sup>6</sup>-mG methyltransferase in the cell line, about 80% of mutations were G:C to A:T transitions. Interestingly, most of the G:C to A:T transition hotspots occur at the second G of the GGT sequence motif, which is the motif of codon 12 in the Ki-ras oncogene [37]. When we define the hotspot as the site where more than four G:C to A:T mutations were identified, we identified 18 hotspots in the *gpt* gene among 155 G:C to A:T mutants recovered from NNK-treated mice. They are nucleotide 27, 64, 86, 87, 92, 107, 110, 113, 115, 116, 128, 274,

281, 287, 402, 409, 417 and 418 when A of ATG of the start codon of the *gpt* gene is set as nucleotide 1. Tiano et al. [36] identified four hotspots of the second G of GGT in nucleotide 23, 116, 128 and 281 in the *gpt* gene, three of which are included in the hotspots identified by us. However, we identified other hotspots such as the second G of GGA at nucleotide 87, 274, 402 and 418, the second G of GGG at nucleotide 27, 64, 92 and 417 and the second G of GGC at nucleotide 113. Thus, we conclude that NNK preferentially induces G:C to A:T mutations at the second G of GGX where X represents any of A, T, G and C. In addition to G:C to A:T and G:C to T:A mutations, we observed an increase in the MFs of A:T to T:A and A:T to C:G in the NNK treated mice (Table 1). Substantial increases in the MFs of A:T to T:A and A:T to C:G are also reported by Hashimoto et al. [38], who examined the genotoxicity of NNK with *lacZ* transgenic mice (Muta<sup>TM</sup> Mouse). Since reporter genes for mutations, such as *gpt*, *cII* or *lacZ*, are not expressed in vivo and are not imposed by any selection bias, they can reflect any genotoxic events occurring in the genomic DNA. In contrast, oncogenes such as the *ras* gene can only detect mutations that can activate the oncogenic activity of the gene products. Thus, we assume that NNK induces modifications in DNA such as O<sup>4</sup>-methyl or O<sup>2</sup>-methyl thymine in the lung, which may account for the induction of A:T to C:G and A:T to T:A mutations, respectively [8]. Although the toxicological significance of these mutations is currently unknown, these mutations may contribute to the carcinogenicity of cigarette smoke as well.

$\gamma$ -Irradiation at dose rate of 1.0 and 1.5 mGy/h clearly enhanced the MFs of large deletions when no NNK treatments were combined (Fig. 3A). The total estimated doses were 0.68 and 1.02 Gy, which may be the lowest radiation doses that gave positive results in transgenic mice mutation assays [16]. In contrast, we could detect no significant increase in the MF of large deletions induced by NNK treatments (Table 2 and Fig. 3A and B). Thus, we suggest that NNK induces mostly base substitutions but not deletions in vivo. Interestingly, NNK treatments induce deletions in cultured mammalian cells. Tiano et al. [36] report that about 20% of mutations induced by NNK treatments are deletions in AS52 hamster cells expressing human CYP2A6. Zhou et al. [31] report that about 80% of NNK-induced mutations are large deletions in the human–hamster hybrid (A<sub>L</sub>) cell assay. We speculate that NNK may have a potential to induce both base substitutions and large deletions in vitro but the latter can be eliminated in vivo by the p53-dependent mechanism. Chinese hamster cell lines such as CHO and V79 harbor missense mutation in the *p53*

gene [39,40]. Large deletions might have been detected in the cultured cells because of inefficient p53 functions.

In summary, we have examined the combined genotoxicity of  $\gamma$ -irradiation and NNK treatments in the lung of *gpt* delta mice. Although radiation did not modulate the NNK-induced base substitutions, NNK treatments suppressed the induction of large deletions in size more than 1 kb induced by the irradiation. NNK treatments might induce an adaptive response, which eliminates the cells bearing radiation-induced DSBs in DNA. This finding may be helpful in understanding the molecular mechanisms of genotoxicity as a result of interactions of more than one genotoxic agents in vivo.

### Acknowledgements

Part of this study was financially supported by the Budget for Nuclear Research of the Ministry of Education, Culture, Sports, Science and Technology, based on the screening and counseling by the Atomic Energy Commission, and the Tutikawa Memorial Fund for Study in Mammalian Mutagenicity.

### References

- [1] R. Doll, R. Peto, The causes of cancer: quantitative estimates of avoidable risks of cancer in the United States today, *J. Natl. Cancer Inst.* 66 (1981) 1191–1308.
- [2] Tobacco smoke and involuntary smoking, IARC Monogr Eval. Carcinog. Risk Chem. Hum., vol. 83, International Agency for Research on Cancer, Lyon, France, 2002.
- [3] S.S. Hecht, Biochemistry, biology, and carcinogenicity of tobacco-specific *N*-nitrosamines, *Chem. Res. Toxicol.* 11 (1998) 559–603.
- [4] S.S. Hecht, Tobacco carcinogens, their biomarkers and tobacco-induced cancer, *Nat. Rev. Cancer* 3 (2003) 733–744.
- [5] International Agency for Research on Cancer Press Release, vol. 154, International Agency for Research on Cancer, Lyon, France, 2004.
- [6] Z.A. Ronai, S. Gradia, L.A. Peterson, S.S. Hecht, G to A transitions and G to T transversions in codon 12 of the *Ki-ras* oncogene isolated from mouse lung tumors induced by 4-(methylnitrosamino)-1-(3-pyridyl)-1-butanone (NNK) and related DNA methylating and pyridyloxobutylating agents, *Carcinogenesis* 14 (1993) 2419–2422.
- [7] R. Guza, M. Rajesh, Q. Fang, A.E. Pegg, N. Tretyakova, Kinetics of *O*<sup>6</sup>-methyl-2'-deoxyguanosine repair by *O*<sup>6</sup>-alkylguanine DNA alkyltransferase within *K-ras* gene-derived DNA sequences, *Chem. Res. Toxicol.* 19 (2006) 531–538.
- [8] E.C. Friedberg, G.C. Walker, W. Siede, R.D. Wood, R.A. Schultz, T. Ellenberger, *DNA Repair and Mutagenesis*, 2nd ed., ASM Press, Washington, DC, 2006, pp. 1–1118.
- [9] United Nations Scientific Committee on the Effects of Atomic Radiation, Sources, Effects and Risks of Ionising Radiation, 1988 Report to the General Assembly with Annexes, United Nations Press, New York, 1989.
- [10] J.H. Lubin, K. Steindorf, Cigarette use and the estimation of lung cancer attributable to radon in the United States, *Radiat. Res.* 141 (1995) 79–85.
- [11] H.P. Leenhouts, M.J. Brugmans, Calculation of the 1995 lung cancer incidence in The Netherlands and Sweden caused by smoking and radon: risk implications for radon, *Radiat. Environ. Biophys.* 40 (2001) 11–21.
- [12] United Nations Scientific Committee on the Effects of Atomic Radiation, Combined Effects of Radiation and Other Agents, Report to the General Assembly, United Nations Press, New York, 1998.
- [13] M.S. Sasaki, Y. Ejima, A. Tachibana, T. Yamada, K. Ishizaki, T. Shimizu, T. Nomura, DNA damage response pathway in radioadaptive response, *Mutat. Res.* 504 (2002) 101–118.
- [14] T. Lindahl, B. Sedgwick, M. Sekiguchi, Y. Nakabeppu, Regulation and expression of the adaptive response to alkylating agents, *Annu. Rev. Biochem.* 57 (1988) 133–157.
- [15] N.G. Oliveira, M. Neves, A.S. Rodrigues, G.O. Monteiro, T. Chaveca, J. Rueff, Assessment of the adaptive response induced by quercetin using the MNCB peripheral blood human lymphocytes assay, *Mutagenesis* 15 (2000) 77–83.
- [16] T. Nohmi, K.I. Masumura, *gpt* Delta transgenic mouse: a novel approach for molecular dissection of deletion mutations in vivo, *Adv. Biophys.* 38 (2004) 97–121.
- [17] T. Nohmi, T. Suzuki, K. Masumura, Recent advances in the protocols of transgenic mouse mutation assays, *Mutat. Res.* 455 (2000) 191–215.
- [18] M. Miyazaki, H. Yamazaki, H. Takeuchi, K. Saoo, M. Yokohira, K. Masumura, T. Nohmi, Y. Funae, K. Imaida, T. Kamataki, Mechanisms of chemopreventive effects of 8-methoxypsoralen against 4-(methylnitrosamino)-1-(3-pyridyl)-1-butanone-induced mouse lung adenomas, *Carcinogenesis* 26 (2005) 1947–1955.
- [19] T. Nohmi, M. Suzuki, K. Masumura, M. Yamada, K. Matsui, O. Ueda, H. Suzuki, M. Katoh, H. Ikeda, T. Sofuni, Spi<sup>-</sup> selection: an efficient method to detect gamma-ray-induced deletions in transgenic mice, *Environ. Mol. Mutagen.* 34 (1999) 9–15.
- [20] K. Masumura, K. Kuniya, T. Kurobe, M. Fukuoka, F. Yatagai, T. Nohmi, Heavy-ion-induced mutations in the *gpt* delta transgenic mouse: comparison of mutation spectra induced by heavy-ion, X-ray, and gamma-ray radiation, *Environ. Mol. Mutagen.* 40 (2002) 207–215.
- [21] T. Nohmi, K. Masumura, Molecular nature of intrachromosomal deletions and base substitutions induced by environmental mutagens, *Environ. Mol. Mutagen.* 45 (2005) 150–161.
- [22] M. Horiguchi, K.I. Masumura, H. Ikehata, T. Ono, Y. Kanke, T. Nohmi, Molecular nature of ultraviolet B light-induced deletions in the murine epidermis, *Cancer Res.* 61 (2001) 3913–3918.
- [23] W. Zhang, C. Wang, D. Chen, M. Minamihisamatsu, H. Morishima, Y. Yuan, L. Wei, T. Sugahara, I. Hayata, Effect of smoking on chromosomes compared with that of radiation in the residents of a high-background radiation area in China, *J. Radiat. Res. (Tokyo)* 45 (2004) 441–446.
- [24] Z.B. Tokarskaya, B.R. Scott, G.V. Zhuntova, N.D. Okladnikova, Z.D. Belyaeva, V.F. Khokhryakov, H. Schollnberger, E.K. Vasilenko, Interaction of radiation and smoking in lung cancer induction among workers at the Mayak nuclear enterprise, *Health Phys.* 83 (2002) 833–846.
- [25] V.E. Archer, Enhancement of lung cancer by cigarette smoking in uranium and other miners, *Carcinog. Compr. Surv.* 8 (1985) 23–37.